

Theoretical characterization of uncertainty in high-dimensional linear classification

Lucas Clarté¹, Bruno Loureiro²,
Florent Krzakala², and Lenka Zdeborová¹

¹ École Polytechnique Fédérale de Lausanne (EPFL), Statistical Physics of Computation lab.,
CH-1015 Lausanne, Switzerland

² École Polytechnique Fédérale de Lausanne (EPFL), Information, Learning and Physics lab.,
CH-1015 Lausanne, Switzerland

Abstract

Being able to reliably assess not only the *accuracy* but also the *uncertainty* of models' predictions is an important endeavour in modern machine learning. Even if the model generating the data and labels is known, computing the intrinsic uncertainty after learning the model from a limited number of samples amounts to sampling the corresponding posterior probability measure. Such sampling is computationally challenging in high-dimensional problems and theoretical results on heuristic uncertainty estimators in high-dimensions are thus scarce. In this manuscript, we characterise uncertainty for learning from limited number of samples of high-dimensional Gaussian input data and labels generated by the probit model. We prove that the Bayesian uncertainty (i.e. the posterior marginals) can be asymptotically obtained by the approximate message passing algorithm, bypassing the canonical but costly Monte Carlo sampling of the posterior. We then provide a closed-form formula for the joint statistics between the logistic classifier, the uncertainty of the statistically optimal Bayesian classifier and the ground-truth probit uncertainty. The formula allows us to investigate calibration of the logistic classifier learning from limited amount of samples. We discuss how over-confidence can be mitigated by appropriately regularising, and show that cross-validating with respect to the loss leads to better calibration than with the 0/1 error.

1 Introduction

An important part of statistics is concerned with assessing the *uncertainty* associated with a prediction based on data. Indeed, in many sensitive fields where statistical methods are widely used, e.g. in medical diagnosis or clinical trials, trustworthiness can be as important as accuracy. The same holds true for modern applications of machine learning where liability is important, e.g. self-driving cars and facial recognition. Yet, assessing uncertainty of machine learning methods comes with many questions. Measuring uncertainty in complex architectures such as deep neural networks is a challenging problem, with a rich literature proposing different strategies, e.g. [17, 28, 23].

On the side of theoretical control of the uncertainty estimators there is an extended work in the context of Gaussian processes [44, 24] that offer Bayesian estimates of uncertainties based on a Gaussian approximation over the predictor class. Essentially when the posterior measure is a high-dimensional Gaussian then computation of the marginals is possible and well controlled. Beyond the setting of Gaussian posterior measures, well-established mathematical guarantees fall short in the high-dimensional regime where the number of data samples is of the same order as the number of dimensions even for the simplest models [45]. Sharp theoretical results on uncertainty quantification in high-dimensional models where posterior distributions are not Gaussian are consequently scarce.

In this manuscript we provide an exact characterisation of uncertainty for high-dimensional classification of data with Gaussian covariates and probit labels. In the model considered here, the uncertainty of the predictions stems from the noise in the data model itself and from the fact that the training data is finite. We are then interested in addressing two questions: a) How does the confidence of the logistic classifier's predictions compares with the intrinsic Bayesian uncertainty when learning with a limited amount of data ? b) How do these two uncertainty measures compare with the true model uncertainty due to the noise in the data model? Although in general computing the Bayesian estimator from posterior sampling can be prohibitively computationally costly in high-dimensions, we show that in the present model it can be efficiently done using a tailored approximate message passing (AMP) algorithm [10, 42]. Leveraging tools from the GAMP literature and its state evolution, we provide an asymptotic characterisation of the joint statistics between the minimiser of the logistic loss, the optimal Bayesian estimator over the data and the oracle estimator. This allows us to provide quantitative answers to questions a) & b) above, and to study how uncertainty estimation depends on the parameters of the model, such as the regularisation, size of the training set and noise.

Main contributions – By order of presentation, the main contributions in this manuscript are:

- We prove that the optimal Bayesian classifier for a data model with Gaussian i.i.d. covariates and probit labels is well approximated (in quadratic time in the input dimension d) by the generalized approximate message passing (AMP) algorithm. In particular, GAMP provides an exact estimation of the Bayesian uncertainty when $d \rightarrow \infty$.
- We provide an exact asymptotic description of the joint statistics between the oracle, Bayes-optimal and logistic classifiers for the aforementioned data model. This allow us to sharply characterise the uncertainty of estimation in high-dimensions, and to evaluate different metrics of interest such as the calibration.
- We prove that the logistic classifier has the same calibration with respect to both the oracle and Bayesian classifiers. However, we show that conditioned on the prediction of the logistic classifier, the variance of the oracle is considerably higher than the Bayesian variance, showing the intrinsic limitations of the calibration as a way to fix the estimation of uncertainty in high-dimensions.
- Finally, we discuss the role played by the ℓ_2 -regularization on uncertainty estimation. In particular, our results suggest that cross-validating with respect to the optimisation loss (logistic) provides a better calibrated classifier than cross-validating with respect to the 0/1 error, while keeping essentially the same test performance.

Related work – Measures of uncertainty: Measuring uncertainty in neural networks is a challenging problem with a vast literature proposing both frequentist and Bayesian approaches [1]. On the frequentist side, various algorithms have been introduced to evaluate and improve the calibration of machine learning models. Some of them, such as isotonic regression [50], histogram binning [49], Platt scaling [40] or temperature scaling [23] are applied to previously trained models. Other approaches aim to calibrate models during training, using well-chosen metrics [39, 29] or through data augmentation [48]. Alternatively, different authors have proposed uncertainty measures based on Bayesian estimates. This includes popular methods such as Bayesian dropout [17, 27], deep ensembles [28, 33, 29] and variational inference [41] to cite a few.

Exact asymptotics: Our theoretical analysis builds on series of developments on the study of exact asymptotics in high-dimensions. The generalised approximate message passing (GAMP) algorithm and the corresponding state evolution equations appeared in [42, 26]. Exact asymptotics for Bayesian estimation in generalised linear models was rigorously established in [9]. On the empirical risk minimisation side, exact asymptotics based on different techniques, such as Convex Gaussian Min-Max Theorem (GMMT) [12, 14, 46, 3, 37, 38, 30], Random Matrix Theory [32], GAMP [19, 31] and first order expansions [11] have been used to study high-dimensional logistic regression and max-margin estimation.

Uncertainty & exact asymptotics: Calibration has been studied in the context of high-dimensional unregularised logistic regression in [6], where it was shown that the logistic classifier is systematically overconfident in the regime where number of samples is proportional to the dimension. An equivalent result for regression

was discussed in [7], where it was shown that quantile regression suffers from an under-coverage bias in high-dimensions.

Notation – Vectors are denoted in bold. $\mathcal{N}(\mathbf{x}|\boldsymbol{\mu}, \Sigma)$ denotes the Gaussian density. \odot denotes the (component-wise) Hadamard product. $\mathbf{1}(A)$ denotes the indicator on the set A .

2 Setting

The data model – Consider a binary classification problem where n samples $(\mathbf{x}^\mu, y^\mu) \in \mathbb{R}^d \times \{-1, 1\}$, $\mu = 1, \dots, n$ are independently drawn from the following probit model:

$$f_\star(\mathbf{x}) := \mathbb{P}(y^\mu = 1|\mathbf{x}^\mu) = \sigma_\star\left(\frac{\mathbf{w}_\star^\top \mathbf{x}^\mu}{\tau}\right),$$

$$\mathbf{x}^\mu \sim \mathcal{N}(\mathbf{0}, \mathbf{I}_d), \quad \mathbf{w}_\star \sim \mathcal{N}(\mathbf{0}, \mathbf{I}_d). \quad (1)$$

where $\sigma_\star(x) = 1/2 \operatorname{erfc}(-x/\sqrt{2})$ and $\tau \geq 0$ parametrises the noise level. Note that the probit model is equivalent to generating the labels via $y^\mu = f_0(\mathbf{w}_\star^\top \mathbf{x}^\mu + \tau \xi^\mu)$ with $\xi^\mu \sim \mathcal{N}(0, 1)$ and $f_0(x) := \operatorname{sign}(x)$. In the following we will be referring to the function $f_\star(\mathbf{x})$ or to its parameters \mathbf{w}_\star as the *teacher*, having in mind the teacher-student setting from neural networks.

Given the training data $\mathcal{D} = \{(\mathbf{x}^\mu, y^\mu)\}_{\mu=1}^n$ and a test sample $\mathbf{x} \sim \mathcal{N}(\mathbf{0}, \mathbf{I}_d)$, the goal is to find a (probabilistic) classifier $x \rightarrow \hat{y}(x)$ minimizing the 0/1 test error

$$\varepsilon_g = \mathbb{E}_{\mathbf{x}, y} \mathbb{P}(\hat{y}(x) \neq y). \quad (2)$$

Considered classifiers – We will focus on comparing two probabilistic classifiers $\hat{f}(\mathbf{x}) = \mathbb{P}(y = 1|\mathbf{x})$. The first is the widely used logistic classifier: $\hat{f}_{\text{erm}}(\mathbf{x}) = \sigma(\hat{\mathbf{w}}_{\text{erm}}^\top \mathbf{x})$ where $\sigma(x) = (1 + e^{-x})^{-1}$ is the logistic function and the weights $\hat{\mathbf{w}} \in \mathbb{R}^d$ are obtained by minimising the following (regularised) empirical risk:

$$\hat{\mathcal{R}}_n(\mathbf{w}) = \frac{1}{n} \sum_{\mu=1}^n \log\left(1 + e^{-y^\mu \mathbf{w}^\top \mathbf{x}^\mu}\right) + \frac{\lambda}{2} \|\mathbf{w}\|_2^2. \quad (3)$$

The second estimator we investigate is the statistically optimal Bayesian estimator for the problem, which is given by:

$$\begin{aligned} \hat{f}_{\text{bo}}(\mathbf{x}) &= \mathbb{P}_{\text{BO}}(y = 1|\mathbf{x}) = \int_{\mathbb{R}^d} d\mathbf{w} P(y = 1|\mathbf{x}^\top \mathbf{w}) P(\mathbf{w}|\mathcal{D}) \\ &= \int_{\mathbb{R}^d} d\mathbf{w} \sigma_\star\left(\frac{\mathbf{w}^\top \mathbf{x}}{\tau}\right) P(\mathbf{w}|\mathcal{D}), \end{aligned} \quad (4)$$

where the posterior distribution $P(\mathbf{w}|\mathcal{D})$ given the training data $\mathcal{D} = \{(\mathbf{x}^\mu, y^\mu)\}_{\mu=1}^n$ is explicitly given by:

$$P(\mathbf{w}|\mathcal{D}) = \frac{1}{\mathcal{Z}(\tau)} \prod_{\mu=1}^n \sigma_\star\left(y^\mu \frac{\mathbf{w}^\top \mathbf{x}^\mu}{\tau}\right) \mathcal{N}(\mathbf{w}|\mathbf{0}, \mathbf{I}_d), \quad (5)$$

for a normalisation constant $\mathcal{Z}(\tau) \in \mathbb{R}$. Note that the Bayes-optimal (BO) estimator assumes the knowledge of the value τ . If τ was not known, under the probit model, it could be learned with expectation maximization as $\tau = \operatorname{argmax}_{\tilde{\tau}} \mathcal{Z}(\tilde{\tau})$, where the normalization $\mathcal{Z}(\tilde{\tau})$ can be estimated asymptotically accurately with the GAMP algorithm.

Uncertainty and calibration – The main purpose of this manuscript is to characterise how the intrinsic uncertainty of the probit model compares to both the Bayesian and logistic confidences/uncertainties in the high-dimensional setting where the number of samples n is comparable to the dimension d . In this case, the limited number of samples is one of the main sources of uncertainty. Note that the corresponding classifier

$\hat{f} = \mathbb{P}(y = 1|\mathbf{x})$ gives the probability that the label $y = 1$ (with the label prediction commonly given by thresholding this function). In mathematical terms, we aim at characterising the correlation between the teacher, Bayesian and logistic confidences, as parametrised by the joint probability density:

$$\rho(a, b, c) = \mathbb{P}_{\mathcal{D}, \mathbf{x}}(f_{\star}(\mathbf{x}) = a, \hat{f}_{\text{bo}}(\mathbf{x}) = b, \hat{f}_{\text{erm}}(\mathbf{x}) = c). \quad (6)$$

Similarly, we will note $\rho_{\star, \text{erm}}(a, c) = \mathbb{P}(f_{\star} = a, \hat{f}_{\text{erm}} = c)$, $\rho_{\text{bo}, \text{erm}}(b, c) = \mathbb{P}(\hat{f}_{\text{bo}} = b, \hat{f}_{\text{erm}} = c)$ and $\rho_{\star, \text{bo}}(a, b) = \mathbb{P}(f_{\star} = a, \hat{f}_{\text{bo}} = b)$. These densities correspond to ρ summed over \hat{f}_{bo} , f_{\star} and \hat{f}_{erm} respectively. Here the sample \mathbf{x} is understood as one from the test set, on which the confidence/uncertainty is evaluated. In the next Section, we provide a characterisation of this joint density in the high-dimensional limit where $n, d \rightarrow \infty$ with fixed sample complexity $\alpha = n/d$, as a function of the noise level τ and regularization λ . To obtain this result we leverage recent works on approximate message passing algorithms and their state evolution.

We also connect our results to the commonly used notion of calibration of a probabilistic classifier $\hat{f} : \mathbb{R}^d \rightarrow [0, 1]$ defined as:

$$\Delta_p(\hat{f}) := p - \mathbb{E}_{\mathbf{x}, y^*}(f_{\star}(\mathbf{x}) | \hat{f}(\mathbf{x}) = p) \quad (7)$$

where \hat{f} can be the logistic classifier or the Bayes-optimal one. Note, however, that the calibration is an average notion, while the above joint probability distribution (6) captures more detailed information about the point-wise confidence and its reliability. In this work, we will also consider the calibration of ERM with respect to Bayes

$$\tilde{\Delta}_p := p - \mathbb{E}_{\mathbf{x}, y^*}(\hat{f}_{\text{bo}}(\mathbf{x}) | \hat{f}_{\text{erm}}(\mathbf{x}) = p) \quad (8)$$

For $p > 1/2$, if the calibration $\Delta_p > 0$ we will say the estimator \hat{f} is overconfident, and when $\Delta_p < 0$ we will say it is underconfident.

3 Main technical results

Our first main result is the existence of an efficient algorithm, called Generalized Approximate Message Passing (GAMP) [42, 26] that is able to accurately estimate $\hat{f}_{\text{bo}}(\mathbf{x})$ in high-dimensions:

Theorem 3.1 (GAMP-Optimality). *For a sequence of problems given by eq. (1), and given the estimator $\hat{\mathbf{w}}_{\text{amp}}$ from algorithm 1, the predictor*

$$\hat{f}_{\text{amp}}(\mathbf{x}) = \mathbb{P}(y = 1|\mathbf{x}) = \sigma_{\star} \left(\frac{\hat{\mathbf{w}}_{\text{amp}}^{\top} \mathbf{x}}{\sqrt{\tau^2 + \hat{\mathbf{c}}_{\text{amp}}^{\top}(\mathbf{x} \odot \mathbf{x})}} \right) \quad (9)$$

achieves Bayes-optimal test performance. Moreover, with high probability over a new sample \mathbf{x} the classifier above is asymptotically equal to the Bayesian estimator $\hat{f}_{\text{bo}}(\mathbf{x}) = \mathbb{P}(y = 1|\mathbf{x}) = \hat{f}_{\text{amp}}(\mathbf{x})$ in eq. (4). More precisely:

$$\lim_{d \rightarrow \infty} \mathbb{E}_{\mathbf{x}, \mathcal{D}} \left[|\hat{f}_{\text{amp}}(\mathbf{x}) - \hat{f}_{\text{bo}}(\mathbf{x})|^2 \right] \rightarrow 0. \quad (10)$$

Proof. First, let us establish the expression of the estimator. The GAMP posterior estimation on the weights \mathbf{w} is Gaussian, with mean $\hat{\mathbf{w}}_{\text{amp}}$ and variance $\hat{\mathbf{c}}_{\text{amp}}$. Given this estimate on the weights, the estimate on the pre-activation for a new sample \mathbf{x} is a Gaussian with mean $\hat{\mathbf{w}}_{\text{amp}} \cdot \mathbf{x}$ and variance $\hat{\mathbf{c}}_{\text{amp}}^{\top}(\mathbf{x} \odot \mathbf{x})$. The label being generated by adding a noise of variance τ^2 and taking the sign, the AMP estimate that the label takes value one is thus given by (denoting $\xi \sim \mathcal{N}(0, 1)$ a Normal random variable):

$$\hat{f}_{\text{amp}}(\mathbf{x}) = \mathbb{P} \left(\xi \geq - \frac{\hat{\mathbf{w}}_{\text{amp}}^{\top} \mathbf{x}}{\sqrt{\hat{\mathbf{c}}_{\text{amp}}^{\top}(\mathbf{x} \odot \mathbf{x}) + \tau^2}} \right). \quad (11)$$

Using the definition of the error function, a change of variables then leads to (9).

Algorithm 1 GAMP

Input: Data $\mathbf{X} \in \mathbb{R}^{n \times d}$, $\mathbf{y} \in \{-1, 1\}^n$
 Pre-processing: Define $\mathbf{X}^2 = \mathbf{X} \odot \mathbf{X} \in \mathbb{R}^{n \times d}$.
 Initialize $\hat{\mathbf{w}}^{t=0} = \mathcal{N}(\mathbf{0}, \sigma_w^2 \mathbf{I}_d)$, $\hat{\mathbf{c}}^{t=0} = \mathbf{1}_d$, $\mathbf{g}^{t=0} = \mathbf{0}_n$.
for $t \leq t_{\max}$ **do**
 /* Update channel mean and variance */
 $\mathbf{V}^t = \mathbf{X}^2 \hat{\mathbf{c}}^t$
 $\mathbf{w}^t = \mathbf{X} \hat{\mathbf{w}}^t - \mathbf{V}^t \odot \mathbf{g}^{t-1}$
 /* Update channel */
 $\mathbf{g}^t = f_{\text{out}}(\mathbf{y}, \mathbf{w}^t, \mathbf{V}^t)$
 $\partial \mathbf{g}^t = \partial_{\omega} f_{\text{out}}(\mathbf{y}, \mathbf{w}^t, \mathbf{V}^t)$
 /* Update prior mean and variance */
 $\mathbf{A}^t = -\mathbf{X}^{2\top} \partial \mathbf{g}^t$
 $\mathbf{b}^t = \mathbf{X}^{\top} \mathbf{g}^t + \mathbf{A}^t \odot \hat{\mathbf{w}}^t$
 /* Update marginals */
 $\hat{\mathbf{w}}^{t+1} = (\mathbf{I}_d + \mathbf{A}^t)^{-1} \mathbf{b}^t$
 $\hat{\mathbf{c}}^{t+1} = (\mathbf{I}_d + \mathbf{A}^t)^{-1}$
end for

Return: Estimators $\hat{\mathbf{w}}_{\text{amp}}, \hat{\mathbf{c}}_{\text{amp}} \in \mathbb{R}^d$

The theorem is then a generic consequence of the optimality of approximate message passing algorithms for high-dimensional linear classification [9]. Indeed, the performance of AMP (predicted by state evolution) is given by the very same equation that predicts the Bayes minimal mean-squared error on new samples. Since this is given by the posterior estimate that $\mathbb{P}(y = 1)$, this implies that the AMP estimation of this probability is asymptotically sharp. More details and the full proof are given in Appendix B. \square

Our second main technical result is a formula for the joint distribution of the teacher label, its Bayes estimate, and the error estimate from empirical risk minimisation defined in eq. (6), described in the following theorem:

Theorem 3.2. Consider training data $\mathcal{D} = \{(\mathbf{x}^{\mu}, y^{\mu})\}_{\mu=1}^n$ sampled from the model defined in eq. (1). Let $\hat{\mathbf{w}}_{\text{erm}} \in \mathbb{R}^d$ be the solution of the empirical risk minimisation (3) and $\hat{\mathbf{w}}_{\text{amp}}$ denote the estimator returned by running algorithm 3.1 on the data \mathcal{D} . Then in the high-dimensional limit where $n, d \rightarrow \infty$ with $\alpha = n/d$ fixed, the asymptotic joint density (6) is given by:

$$\rho(a, b, c) = \tau' \tau \frac{\mathcal{N} \left(\begin{bmatrix} \tau \cdot \sigma_{\star}^{-1}(a) \\ \tau' \cdot \sigma_{\star}^{-1}(b) \\ \sigma^{-1}(c) \end{bmatrix} \middle| \mathbf{0}_3, \Sigma \right)}{|\sigma'_{\star}(\sigma_{\star}^{-1}(a))| |\sigma'_{\star}(\sigma_{\star}^{-1}(b))| |\sigma'(\sigma^{-1}(c))|} \quad (12)$$

where we noted

$$\tau'^2 = \tau^2 + 1 - q_{\text{bo}}, \quad \Sigma = \begin{bmatrix} 1 & q_{\text{bo}} & m \\ q_{\text{bo}} & q_{\text{bo}} & m \\ m & m & q_{\text{erm}} \end{bmatrix} \quad (13)$$

and the so-called overlaps:

$$q_{\text{bo}} = \frac{1}{d} \hat{\mathbf{w}}_{\text{amp}}^{\top} \mathbf{w}_{\star} = \frac{1}{d} \|\hat{\mathbf{w}}_{\text{amp}}\|_2^2 \quad (14)$$

$$m = \frac{1}{d} \hat{\mathbf{w}}_{\text{erm}}^{\top} \mathbf{w}_{\star}, \quad q_{\text{erm}} = \frac{1}{d} \|\hat{\mathbf{w}}_{\text{erm}}\|_2^2 \quad (15)$$

solve the following set of self-consistent equations:

$$\frac{1}{q_{\text{bo}}} = 1 + \alpha \mathbb{E}_{(z, \eta), \xi} [f_{\text{out}}(f_0(z + \tau \xi), \eta, 1 - q_{\text{bo}})^2], \quad (16)$$

and

$$V = \frac{1}{\lambda + \hat{V}}, \quad q_{\text{erm}} = \frac{\hat{m}^2 + \hat{q}}{(\lambda + \hat{V})^2}, \quad m = \frac{\hat{m}}{\lambda + \hat{V}}. \quad (17)$$

$$\begin{cases} \hat{V} &= -\alpha \mathbb{E}_{(z, \omega), \xi} [\partial_\omega f_{\text{erm}}(f_0(z + \tau\xi), \omega, V)] \\ \hat{q} &= \alpha \mathbb{E}_{(z, \omega), \xi} [f_{\text{erm}}(f_0(z + \tau\xi), \omega, V)^2] \\ \hat{m} &= \alpha \mathbb{E}_{(z, \omega), \xi} [f_{\text{erm}}(f_0(z + \tau\xi), \omega, V)] \end{cases} \quad (18)$$

where $(z, \eta, \omega) \sim \mathcal{N}(0_3, \Sigma)$, $\xi \sim \mathcal{N}(0, 1)$ and the thresholding functions are defined as

$$\begin{aligned} f_{\text{out}}(y, \omega, V) &= \frac{2y \mathcal{N}(\omega y | 0, V + \tau^2)}{\text{erfc} \left(-\frac{y\omega}{\sqrt{2(\tau^2 + V)}} \right)} \\ f_{\text{erm}}(y, w, V) &= V^{-1} \left(\text{prox}_{Vl(y, \cdot)}(w) - w \right) \end{aligned} \quad (19)$$

with $\text{prox}_{\tau f}(x) = \arg\min_z (1/2\tau \|z - x\|_2^2 + f(z))$ being the proximal operator.

Proof. In Appendix A we show how this result can be deduced directly from the heuristic cavity method, and the analysis of the GAMP state evolution. Indeed, the ERM estimator can also be obtained from a GAMP algorithm with suitably chosen denoising functions corresponding to the loss function and regularisation term. Therefore, the key idea of our cavity computation is to derive the state evolution for the two GAMP algorithms run in parallel on the same data set \mathcal{D} . This allow us to characterize the joint distribution between the two predictors.

While the state evolution of this joint optimisation program could be directly proven as well (it is a generic consequence of the recent extension of state evolution theorems for AMP in [20]), we follow a slightly different route for the proof, leveraging instead the results of [26, 47, 9, 30].

As discussed in lemma B.3 in the supplement, the activations are described by the joint random variables (over \mathbf{x} and for a fixed set of data) $\nu = \mathbf{x} \cdot \mathbf{w}_*$, $\lambda_{\text{erm}} = \mathbf{x} \cdot \hat{\mathbf{w}}_{\text{erm}}$, $\lambda_{\text{amp}} = \mathbf{x} \cdot \hat{\mathbf{w}}_{\text{amp}}$, as $\mathbb{P}(\nu, \lambda_{\text{erm}}, \lambda_{\text{amp}}) = \mathcal{N}(0, \Sigma)$, with

$$\Sigma = \begin{pmatrix} \frac{\mathbf{w}_* \cdot \mathbf{w}_*}{d} & \frac{\mathbf{w}_* \cdot \hat{\mathbf{w}}_{\text{amp}}}{d} & \frac{\mathbf{w}_* \cdot \hat{\mathbf{w}}_{\text{erm}}}{d} \\ \frac{\hat{\mathbf{w}}_{\text{amp}} \cdot \mathbf{w}_*}{d} & \frac{\hat{\mathbf{w}}_{\text{amp}} \cdot \hat{\mathbf{w}}_{\text{amp}}}{d} & \frac{\hat{\mathbf{w}}_{\text{amp}} \cdot \hat{\mathbf{w}}_{\text{erm}}}{d} \\ \frac{\hat{\mathbf{w}}_{\text{erm}} \cdot \mathbf{w}_*}{d} & \frac{\hat{\mathbf{w}}_{\text{erm}} \cdot \hat{\mathbf{w}}_{\text{amp}}}{d} & \frac{\hat{\mathbf{w}}_{\text{erm}} \cdot \hat{\mathbf{w}}_{\text{erm}}}{d} \end{pmatrix} \quad (20)$$

The main technical challenge is thus to establish the asymptotic correlation between these quantities.

Both the ERM and GAMP Bayes estimators are well under rigorous mathematical control: q_{bo} , the Bayes optimal overlap, as defined in (14), is asymptotically given by the fixed point of (16) [9]. Similarly, the ERM overlaps in eqs. (15) are asymptotically given by the fixed points of equations (17), (18), (19) [3, 16, 30]. Additionally, since these are overlaps given by GAMP, they are correct not only on average, but with high probability for a single instance as $d \rightarrow \infty$ [26].

We are thus only left with the task of estimating the correlation between the GAMP and ERM estimators:

$$Q \equiv \frac{1}{d} \hat{\mathbf{w}}_{\text{amp}} \cdot \hat{\mathbf{w}}_{\text{erm}}. \quad (21)$$

As it turns out, one can show that —due to the optimality of AMP— $\hat{\mathbf{w}}_{\text{amp}}$ is very close to $\hat{\mathbf{w}}_{\text{bo}}$. An application of the Bayes formula then leads to

$$Q = \frac{1}{d} \hat{\mathbf{w}}_{\text{bo}} \cdot \hat{\mathbf{w}}_{\text{erm}} = \frac{1}{d} \mathbf{w}_* \cdot \hat{\mathbf{w}}_{\text{erm}} = m, \quad (22)$$

an example of a Nishimori identity in statistical physics [25, 51]. From this, one can then obtain the covariance of the jointly Gaussian distribution of the Bayes, ERM and teacher pre-activation, leading to (6). More details, as well as the formal proof, are given in Appendix B. \square

Our third theorem is an asymptotic expression for the calibration error.

Theorem 3.3. *The analytical expression of the joint density ρ yields the following expression for the calibration Δ_p :*

$$\Delta_p(\hat{f}_{\text{erm}}) = p - \sigma_{\star} \left(\frac{-\frac{m}{q_{\text{erm}}} \times \sigma^{-1}(p)}{\sqrt{1 - \frac{m^2}{q_{\text{erm}}} + \tau^2}} \right). \quad (23)$$

Moreover, the Bayesian classifier is always well calibrated with respect to the teacher, meaning:

$$\forall p \in [0, 1], \quad \Delta_p(\hat{f}_{\text{bo}}) = 0. \quad (24)$$

Additionally, the calibration of ERM with respect to the Bayesian classifier and the teacher are equal:

$$\forall p \in [0, 1], \quad \Delta_p(\hat{f}_{\text{erm}}) = \tilde{\Delta}_p. \quad (25)$$

Proof. While details of the proof of Theorem 3.3 are provided in appendix B.3, we shall give a brief sketch here. The general idea is the following: computing Δ_p and $\tilde{\Delta}_p$ amounts to computing the expectations $\mathbb{E}(f_{\star}|\hat{f}_{\text{erm}})$ and $\mathbb{E}(\hat{f}_{\text{bo}}|\hat{f}_{\text{erm}})$. However, f_{\star} , \hat{f}_{erm} , \hat{f}_{bo} are deterministic functions of the pre-activation, which as we have shown are jointly Gaussian. So, we deduce that the calibration can be expressed as the expectation of a function of a Gaussian variable. Therefore, the calibration is a function only of the covariance matrix Σ previously introduced, and the theorem follows. \square

Equation (25) provides a recipe to compute the calibration Δ_p in the high-dimensional limit from the knowledge of the data model (1) only, but without knowing the specific realisation of the weights w_{\star} . This is because the quantities q_{bo} , q_{erm} and m self-average as $n, d \rightarrow \infty$, we then obtain the calibration Δ_p without knowing the realisation of w_{\star} .

4 Consequences for uncertainty estimation

4.1 Bayes versus teacher uncertainty

We now discuss the consequences of the theorems from Section 3. Figure 1 left panel depicts the theoretical prediction of the joint density $\rho_{\text{bo},\star}$, between the Bayes posterior confidence/uncertainty \hat{f}_{bo} (x-axes) and the intrinsic confidence/uncertainty of the teacher f_{\star} (y-axes). We see (after inspection of the equations or their evaluation) that the density is positive in the whole support, it is peaked around $(0, 0)$ and $(1, 1)$, but has a notable weight around the diagonal as well. The relatively large spread of the joint density is a consequence of the fact that on top of the intrinsic uncertainty of the teacher, the learning is only done with $n = \alpha d$ samples which causes an additional source of uncertainty captured in the Bayes estimator.

The blue curve is the mean of f_{\star} conditioned on the values of \hat{f}_{bo} . The difference between this and the diagonal is the calibration Δ_p defined in Equation (7). We see that the figure illustrates $\Delta_p(\hat{f}_{\text{bo}}) = 0$, i.e. the Bayesian prediction is well calibrated, as predicted by Theorem 3.3.

The theoretically derived density (Figure 1 left panel) is compared to its numerical estimation in Figure 1 right panel, computed numerically using the GAMP algorithm. To estimate the numerical density in the right panel, we proceed as follow: after fixing the dimension d and the number of training samples $n = \alpha d$, GAMP is ran on the training set. Once GAMP estimators have been obtained, n_{test} test samples are drawn and for each of them we compute the confidence of the teacher $f_{\star}(\mathbf{x})$ from eq. (1), and the Bayesian confidence $\hat{f}_{\text{bo}}(\mathbf{x}) = \hat{f}_{\text{amp}}(\mathbf{x})$ from Theorem 3.1. Finally we plot the histogram of the thus obtained joint density $\rho_{\text{bo},\star}$ over the test samples. As the figure shows, there is a perfect agreement between theory and finite instance simulations.

Figure 2 then depicts the same densities as Figure 1 for several different values of the sample complexity α and noise τ . The corresponding test error is given for information. We see, for instance, that at small α the BO confidence is low, close to 0.5, because not much can be learned from very few samples. The teacher confidence does not depend on α , and is low for growing τ . At large α , on the other hand, the BO confidence is getting well correlated with the teacher one. At larger α and small noise the BO test error is getting smaller and the corresponding confidence close to 1 or 0 (depending on the label).

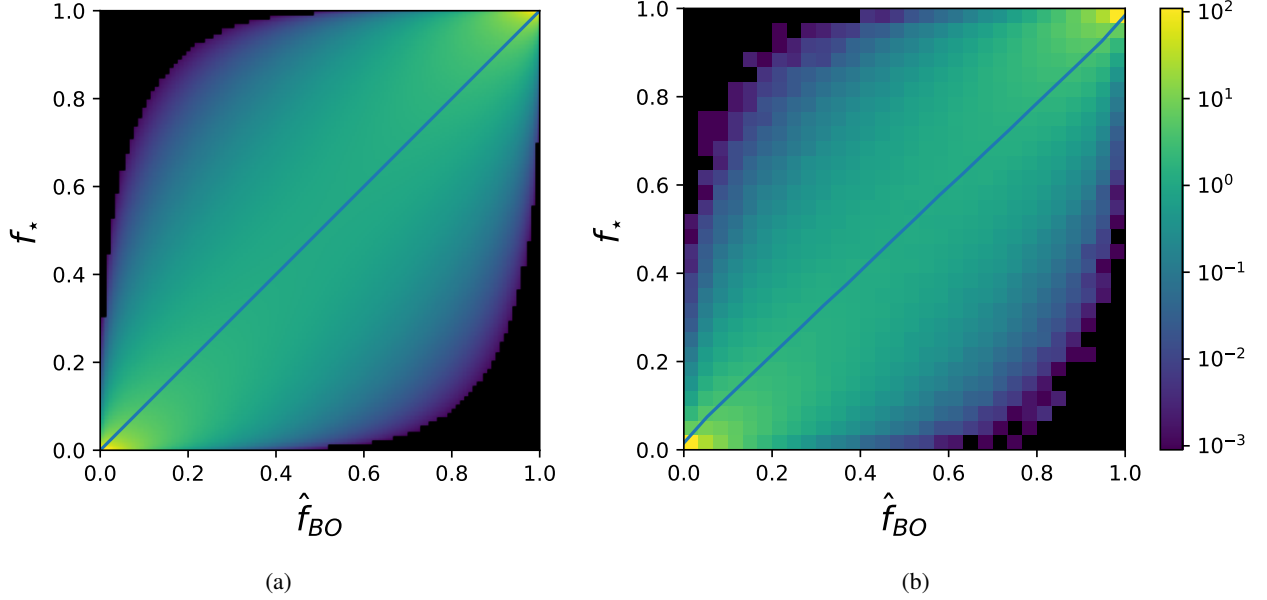


Figure 1: Theoretical prediction (left panel) and numerical estimation (right panel) of the joint density $\rho_{bo,*}$ at $\alpha = 10$ and noise level $\tau = 0.5$. Numerical plot was done by running GAMP at dimension $d = 1000$, computing (f_*, \hat{f}_{bo}) on $n_{\text{test}} = 10^7$ test samples. The blue curve is the mean of f_* given \hat{f}_{bo} . For these parameters, the test error of Bayes is $\varepsilon_g^{\text{bo}} = 0.173$, the oracle test error $\varepsilon^* = 0.148$.

4.2 Logistic regression uncertainty and calibration

Having explicit access to the Bayesian confidence/uncertainty in a high-dimensional setting is a unique occasion to thoroughly investigate the properties of the logistic classifier, which has its own measure of confidence induced by the logit. We start with the logistic classifier at zero regularization and then move to the regularised case in the next section.

Figure 3 compares the joint density of $(\hat{f}_{\text{erm}}, f_*)$ (left panel), and $(\hat{f}_{\text{erm}}, \hat{f}_{bo})$ (right panel) with the same noise and number of samples as used in figure 1. The blue curves are the means of f_* (respectively \hat{f}_{bo}) conditioned on \hat{f}_{erm} . The equality between these two blue curves illustrates Theorem 3.3, Equation (25): $\Delta_p(\hat{f}_{\text{erm}}) = \tilde{\Delta}_p$. Note, however, that while the calibrations of the ERM with respect to the teacher or the BO are equal, the conditional variances of f_* and \hat{f}_{bo} are very different. This shows how the calibration is only a very partial fix of the confidence estimation for ERM: when $\hat{f}_{\text{erm}} = p$, both Bayes and the teacher's predictions will be $p - \Delta_p$ on average, but for the considered parameters the predictions of the teacher are much more spread around this value than those of Bayes estimator.

Let us now investigate the calibration as a function of the sample complexity α . The plot (a) of figure 4 shows the curve Δ_p at $\lambda = 0$ computed using the analytical expression (23). The curve is compared to the numerical estimation of Δ_p (green crosses) and $\tilde{\Delta}_p$ (orange crosses). Δ_p is estimated experimentally with the formula

$$\Delta_p \simeq p - \frac{\sum_{i=1}^{n_{\text{test}}} f_*(x_i) \mathbf{1}(\hat{f}_{\text{erm}}(x_i) \in [p, p + dp])}{\sum_{i=1}^{n_{\text{test}}} \mathbf{1}(\hat{f}_{\text{erm}}(x_i) \in [p, p + dp])} \quad (26)$$

for some small dp . Similarly, $\tilde{\Delta}_p$ can be estimated with

$$\tilde{\Delta}_p \simeq p - \frac{\sum_{i=1}^{n_{\text{test}}} \hat{f}_{bo}(x_i) \mathbf{1}(\hat{f}_{\text{erm}}(x_i) \in [p, p + dp])}{\sum_{i=1}^{n_{\text{test}}} \mathbf{1}(\hat{f}_{\text{erm}}(x_i) \in [p, p + dp])}. \quad (27)$$

The calibrations Δ_p and $\tilde{\Delta}_p$ are both equal to the theoretical curve, further confirming the results of Equation (25). Note the transition at $\alpha_c \sim 2.4$: for $\alpha < \alpha_c$, the training data is linearly separable. Since $\lambda = 0$, the

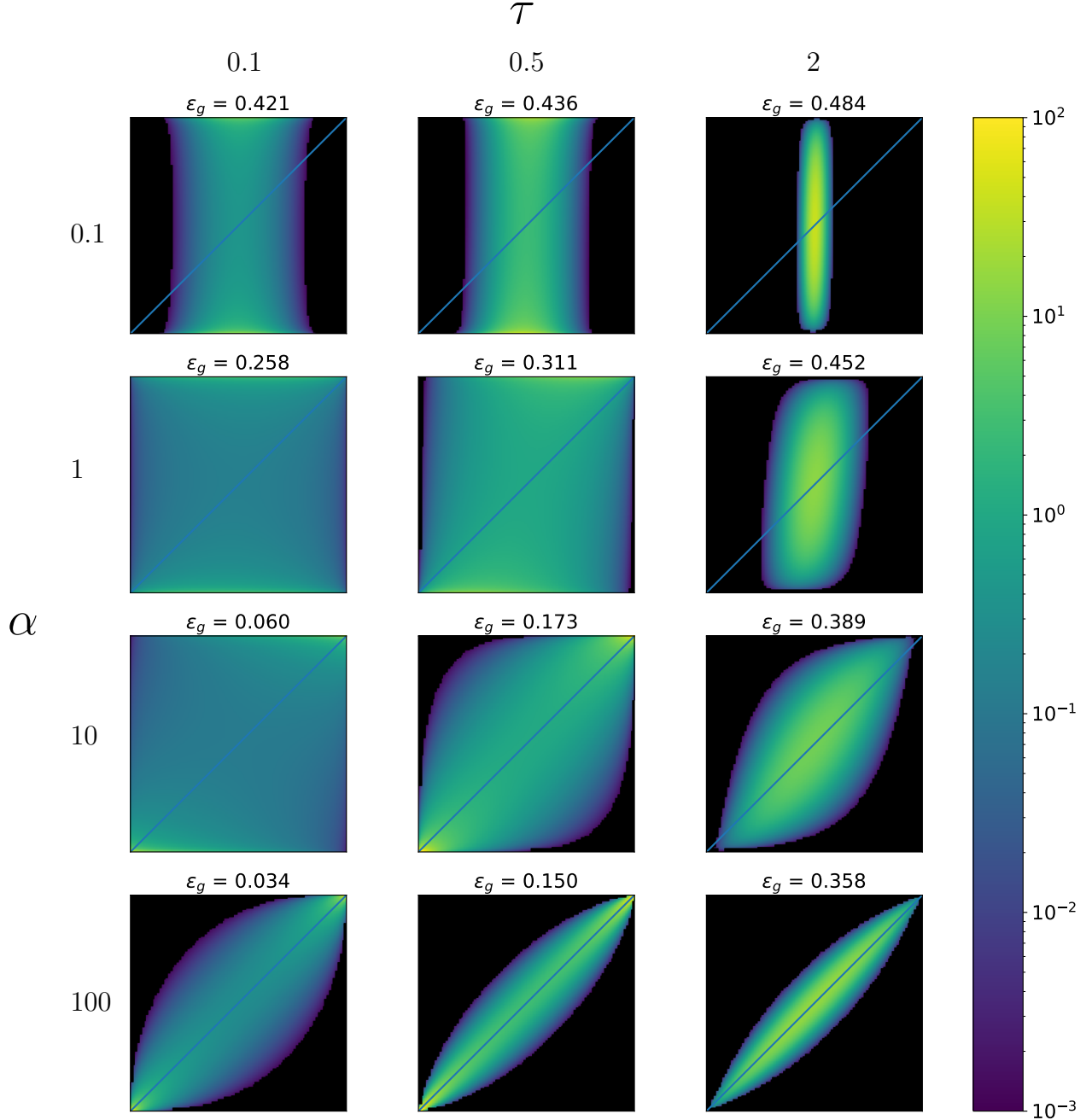


Figure 2: Density between Bayes confidence \hat{f}_{bo} (x-axis) and the teacher confidence f_* (y-axis) for multiple values of α, τ : the rows correspond respectively to $\alpha = 0.1, 1, 10, 100$ from top to bottom, and the columns correspond respectively to $\tau = 0.1, 0.5, 2$. Generalisation errors of the Bayes estimator are in written on top of the corresponding plot. The best possible generalisation errors, achieved if the teacher weights are known, for $\tau = 0.1, 0.5, 2$ are respectively $\varepsilon_g^* = 0.032, 0.148, 0.352$.

empirical risk has no minimum and the estimator \mathbf{w}_{erm} diverges in norm. This amounts to writing $m = \eta m_0$ and $q = \eta^2 q_{\text{erm}0}$ and $\eta \rightarrow \infty$. Plugging this into Equation (23), we see that as $\eta \rightarrow \infty$, $\Delta_p \rightarrow p - 0.5$, as we observe in the plot.

Right panel of figure 4 displays the variance of f_* and \hat{f}_{bo} at fixed \hat{f}_{erm} as a function of α . This plot illustrates that the conditional variance of f_* is significantly higher than that of \hat{f}_{bo} , as was previously noted in figure 3.

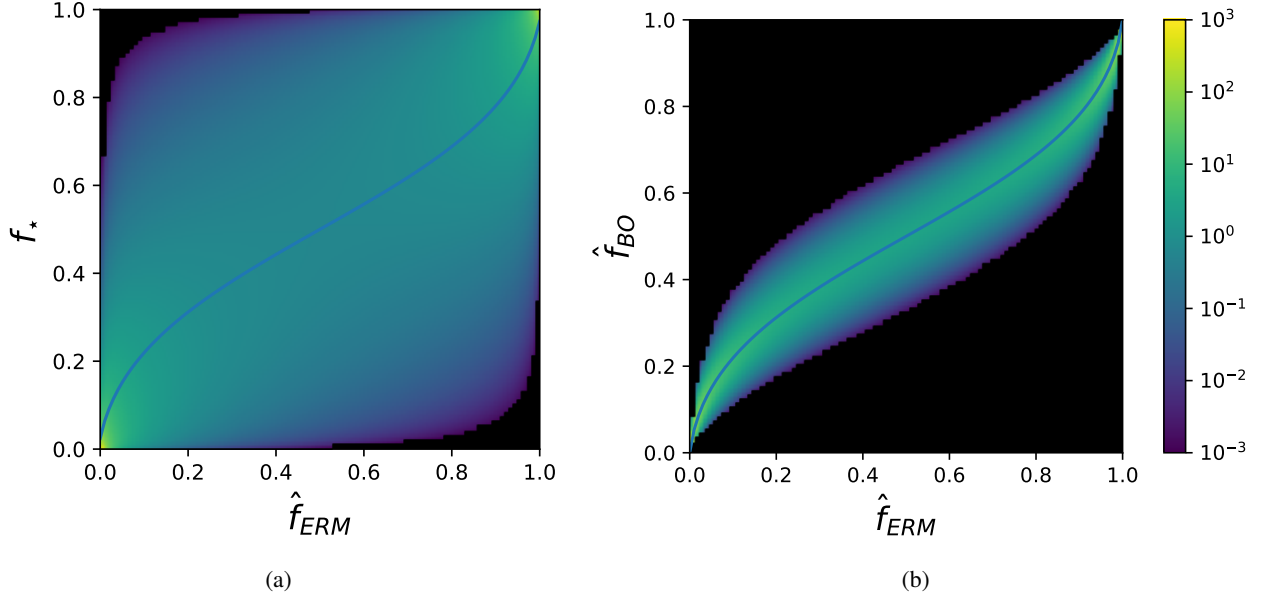


Figure 3: The probability density $\rho_{\text{erm},*}$ (left panel) and $\rho_{\text{erm},\text{bo}}$ (right panel), at $\alpha = 10$, $\tau = 0.5$ and $\lambda = 0$. The blue curves are the mean of the marginal distribution of f_* and \hat{f}_{bo} respectively under fixed \hat{f}_{erm} , which are equal to $p - \Delta_p$ and $p - \hat{\Delta}_p$. We observe overconfidence of the logistic classifier for these parameters. Test error of ERM is here $\varepsilon_g^{\text{erm}} = 0.174$, very close to the one of BO $\varepsilon_g^{\text{bo}} = 0.173$.

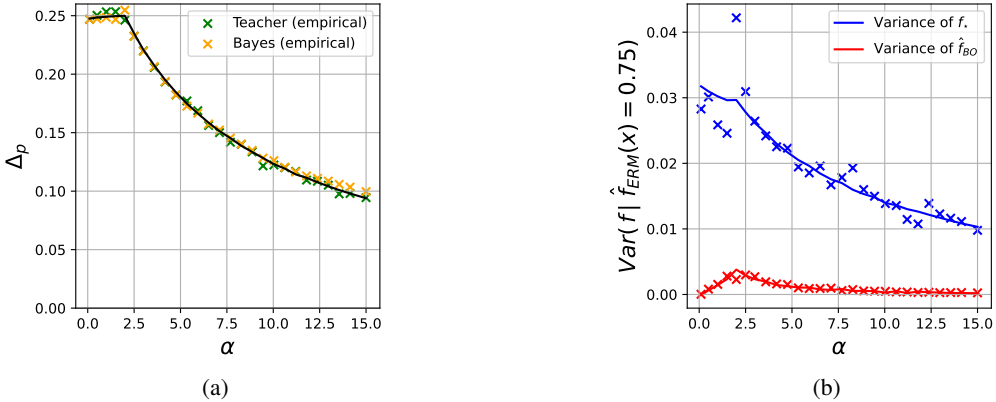


Figure 4: (a) Calibration of the logistic regression with $\lambda = 0, \tau = 2, p = 0.75$. Orange (respectively green) crosses are numerical estimation of $\hat{\Delta}_p$ (respectively Δ_p). Numerical values are obtained by averaging the calibration over 10 test sets of size $n_{\text{test}} = 10^5$, at $d = 300$. (b) Variance of f_* and \hat{f}_{bo} conditioned on $\hat{f}_{\text{ERM}} = p = 0.75$. Crosses are numerical values with the same parameters as figure (a). Though both f_* and \hat{f}_{bo} have the same mean, their variance are significantly different. Making the logistic regression more comparable with the BO estimator than with the teacher.

4.3 Choosing regularization optimally

Logistic regression is rarely used in practice without regularization. One usually optimizes the strength λ of the ℓ_2 penalty through cross-validation by minimizing the validation error. Ideally, we would choose λ that gives a low validation error but also that yields a well-calibrated estimator. We will denote λ_{error} (respectively λ_{loss}) the parameter that minimises the 0/1 classification error (respectively the logistic loss) on the validation set. In the setting of the present paper, these two values of regularisation lead to a very close test error/loss. In other words, choosing one or another of these λ seems to have little effect on the test performance of logistic regression.

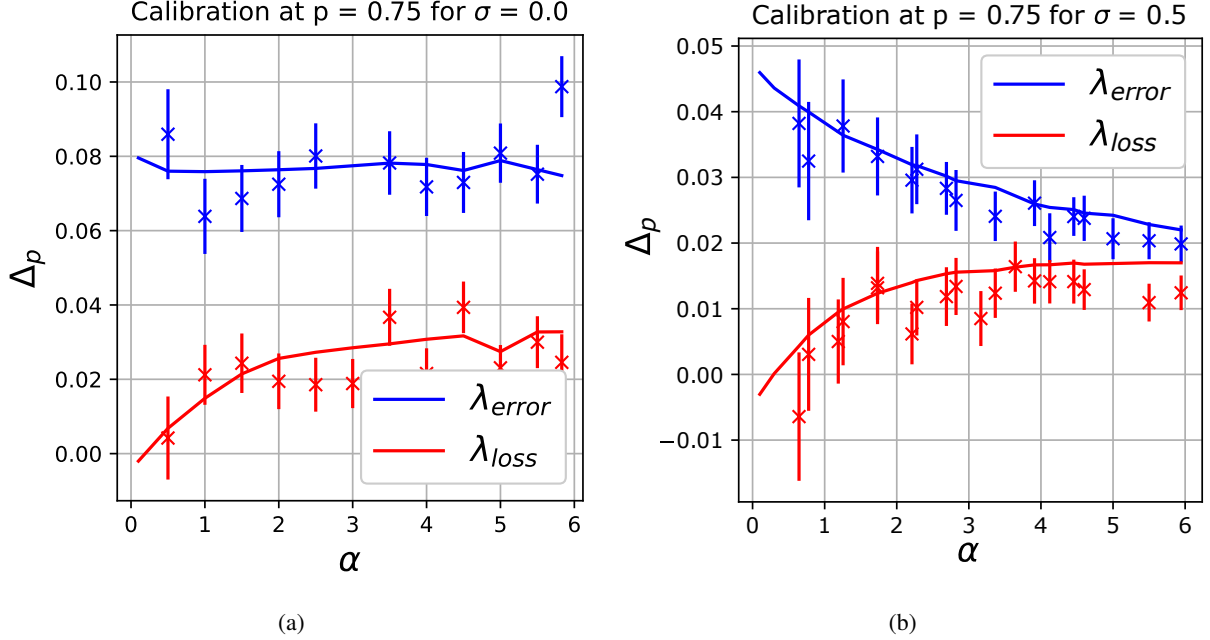


Figure 5: The calibration $\Delta_{0.75}(\hat{f}_{\text{erm}})$ as a function of α with $\lambda = \lambda_{\text{error}}(\alpha, \tau)$ (blue curve) and $\lambda = \lambda_{\text{loss}}(\alpha, \tau)$ (red curve). We see the red curve is closer to zero, thus the estimator is better calibrated at λ_{loss} . Experiments are done using $d = 300$, $n_{\text{test}} = 10^5$ test samples and 1000 trials. In (a), $\tau = 0$; in (b), $\tau = 0.5$.

Figure 5 plots the calibration Δ_p in the noiseless (left panel) and noisy (right panel) settings. We observe that ERM with λ_{loss} is significantly less overconfident than with λ_{error} . In the range of parameters that we used, this choice of penalization λ_{loss} leads to a classifiers that are better calibrated, in addition to having near-optimal performance. We also note that for small α the logistic regression at λ_{loss} even gets mildly underconfident, $\Delta_p < 0$.

In figure 6, we have plotted the density of Bayes and ERM uncertainty evaluated at λ_{error} and λ_{loss} . Comparing the upper panels to Figure 3 (at $\lambda = 0$), it is clear that choosing λ to optimize the error (and the loss) improves calibration. In the lower panels of figure 6 we can also see that the calibration at λ_{loss} (right panel) is better, i.e. the blue line is closer to $y = x$, than the one at λ_{error} (left panel).

In figure 7, the calibration Δ_p is shown as a function of λ at different levels p and different noise σ . First observe that as λ grows the logistic regression is going from overconfident $\Delta_p > 0$ to underconfident $\Delta_p < 0$. For $\lambda \rightarrow \infty$, we have $\Delta_p \rightarrow p - 1$, and as $\lambda \rightarrow 0$, $\Delta_p \rightarrow p - 0.5$. Further, we observe that the value of λ at which the calibration is zero (the best calibration) has only mild dependence on the value of p . Finally, the vertical lines mark the values of regularization that minimize the validation error λ_{error} , and loss λ_{loss} . We see that λ_{loss} is closer to the well-calibrated region, and that at small α this difference is more pronounced.

We thus conclude that in our setting with a probit teacher, using λ_{loss} is clearly advantageous to obtain better calibrated classification. It remains to be investigated whether this is true in more realistic settings. The code of this project is available at <https://github.com/lclarke/uncertainty-project>

5 Discussion

This paper leverages on the properties of the GAMP algorithm and associated closed-form control of the posterior marginals to provide detailed theoretical analysis of uncertainty in a simple probit model. We investigate the relations between the respective uncertainties of the oracle, Bayes and regularized logistic regression. We see this as a first grounding step for a line of future work that will leverage recent extensions of the GAMP algorithm and its associated analysis to multi-layer neural networks [4, 20], learning with random features and kernels [34, 18, 15], estimation under generative priors [5, 2], classification on more realistic models of data [21, 22, 43], etc.

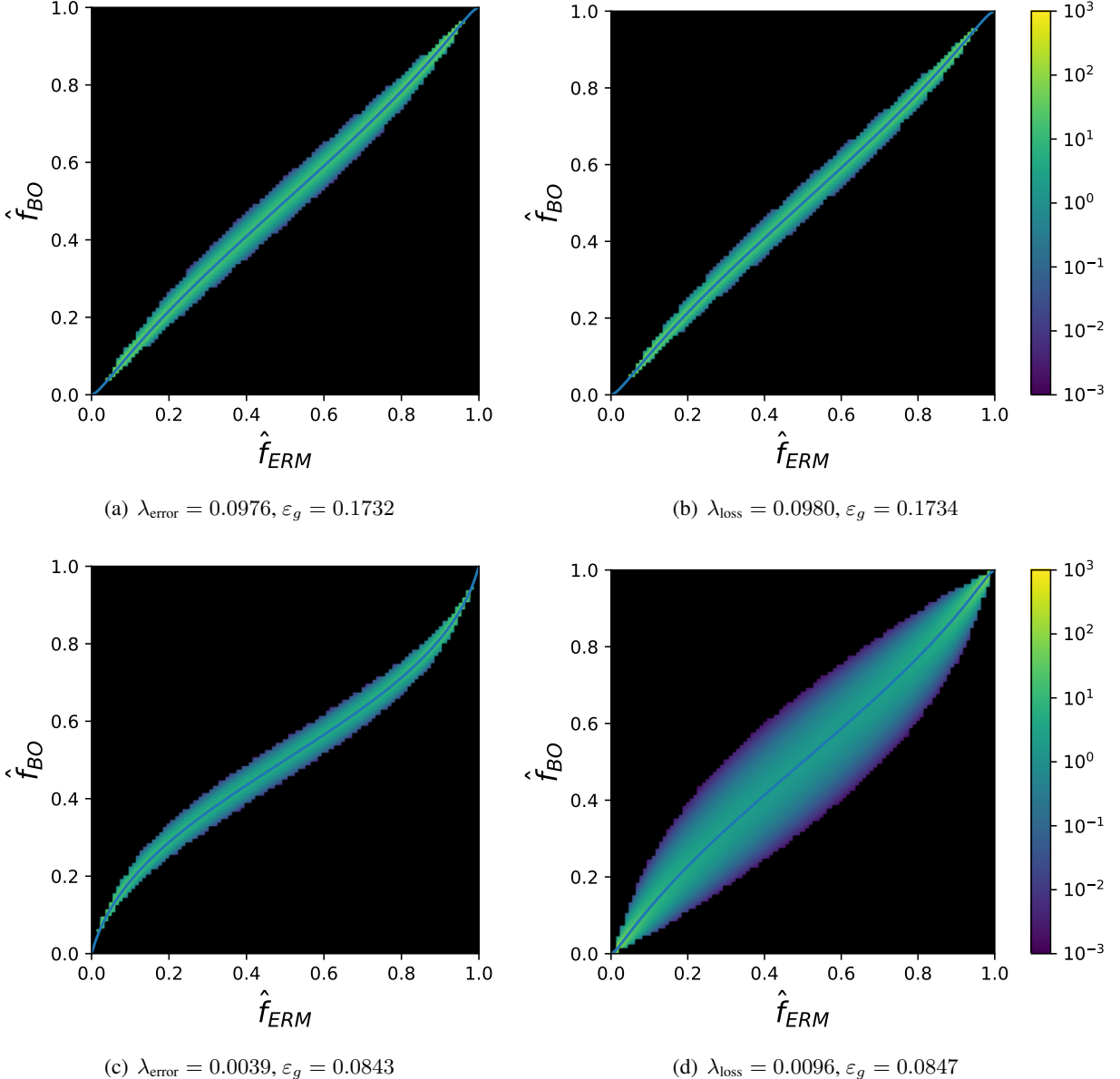


Figure 6: Density $\rho_{\text{erm,bo}}$ for different α, τ . Top row: $\alpha = 10, \tau = 0.5$. Bayes test error is $\varepsilon_g^{\text{bo}} = 0.1731$. Plot (a) (respectively (b)) is done at $\lambda = \lambda_{\text{error}}$ (respectively $\lambda = \lambda_{\text{loss}}$). Bottom row: $\alpha = 5, \tau = 0, \varepsilon_g^{\text{bo}} = 0.0839$. Plot (c) (respectively (d)) is done at $\lambda = \lambda_{\text{error}}$ (respectively $\lambda = \lambda_{\text{loss}}$). On the bottom row, we can clearly see that the calibration is better for λ_{loss} . Generalization errors of ERM as well as the values of the regularizations are indicated below the plots.

In future work we will also study and evaluate more advanced uncertainty estimators, some of those listed in the introduction, in settings where the present methodology gives us a asymptotically exact access to the true Bayesian uncertainty. The present methodology is not restricted to classification and can be also used for more thorough study of confidence intervals in high-dimensional regression, extending [7]. This is left for further studies.

Acknowledgements— We thank Cédric Gerbelot for useful discussion and Benjamin Aubin for his help on the numerical experiments. We acknowledge funding from the ERC under the European Union’s Horizon 2020 Research and Innovation Programme Grant Agreement 714608-SMiLe.

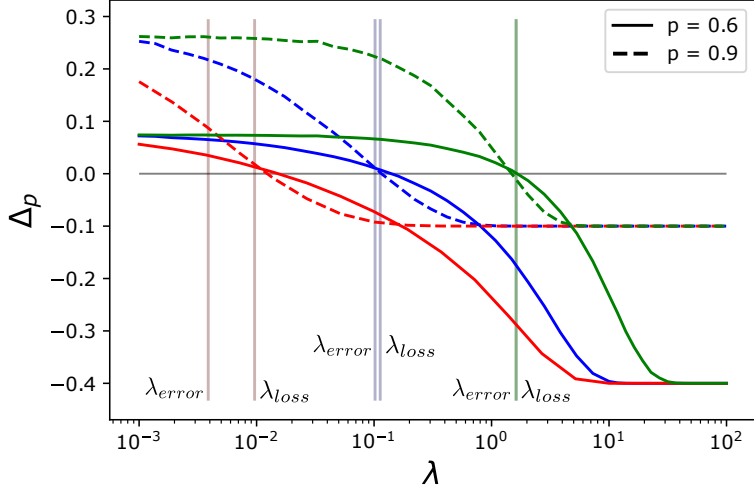


Figure 7: Calibration Δ_p for $p = 0.9$ and $p = 0.6$ as a function of λ , for $\tau = 0$ (red curve), $\tau = 0.5$ (blue curve), and $\tau = 2$ (green curve), at $\alpha = 5$. Vertical lines correspond to λ_{error} and λ_{loss} defined in 4.3. For $\tau = 2$, λ_{error} and λ_{loss} differ by only 10^{-2} and look indistinguishable on the plot.

References

- [1] Moloud Abdar et al. ‘A review of uncertainty quantification in deep learning: Techniques, applications and challenges’. In: *Information Fusion* 76 (2021).
- [2] Benjamin Aubin et al. ‘Exact asymptotics for phase retrieval and compressed sensing with random generative priors’. In: *Proceedings of The First Mathematical and Scientific Machine Learning Conference*. Ed. by Jianfeng Lu and Rachel Ward. Vol. 107. Proceedings of Machine Learning Research. PMLR, July 2020, pp. 55–73.
- [3] Benjamin Aubin et al. ‘Generalization error in high-dimensional perceptrons: Approaching Bayes error with convex optimization’. In: *Advances in Neural Information Processing Systems* (2020). Ed. by H. Larochelle et al., pp. 12199–12210.
- [4] Benjamin Aubin et al. ‘The committee machine: computational to statistical gaps in learning a two-layers neural network’. In: *Journal of Statistical Mechanics: Theory and Experiment* 2019.12 (2019).
- [5] Benjamin Aubin et al. ‘The Spiked Matrix Model With Generative Priors’. In: *IEEE Transactions on Information Theory* 2 (2021).
- [6] Yu Bai, Song Mei and Caiming Xiong. ‘Don’t Just Blame Over-parametrization for Over-confidence: Theoretical Analysis of Calibration in Binary Classification’. In: *arXiv:2102.07856 [cs.LG]* (2021).
- [7] Yu Bai et al. ‘Understanding the Under-Coverage Bias in Uncertainty Estimation’. In: *arXiv:2106.05515 [cs.LG]* (2021).
- [8] Jean Barbier and Nicolas Macris. ‘The adaptive interpolation method: a simple scheme to prove replica formulas in Bayesian inference’. In: *Probability theory and related fields* 174 (2019).
- [9] Jean Barbier et al. ‘Optimal Errors and Phase Transitions in High-Dimensional Generalized Linear Models’. In: *Proceedings of the National Academy of Sciences* 116.12 (2019).
- [10] Mohsen Bayati and Andrea Montanari. ‘The LASSO risk for gaussian matrices’. In: *IEEE Transactions on Information Theory* (2015).
- [11] Pierre Bellec and Arun Kuchibhotla. ‘First order expansion of convex regularized estimators’. In: *Advances in Neural Information Processing Systems*. Ed. by H. Wallach et al. Vol. 32. Curran Associates, Inc., 2019.
- [12] Emmanuel J. Candès and Pragya Sur. ‘The phase transition for the existence of the maximum likelihood estimate in high-dimensional logistic regression’. In: *arXiv:1804.09753 [stat.ME]* (2018).

- [13] M Cover Thomas and A Thomas Joy. ‘Elements of information theory’. In: *New York: Wiley* 3 (1991).
- [14] Zeyu Deng, Abla Kammoun and Christos Thrampoulidis. ‘A Model of Double Descent for High-Dimensional Logistic Regression’. In: *ICASSP 2020 - 2020 IEEE International Conference on Acoustics, Speech and Signal Processing (ICASSP)*. 2020.
- [15] Oussama Dhifallah and Yue M Lu. ‘A precise performance analysis of learning with random features’. In: *arXiv:2008.11904 [cs.IT]* (2020).
- [16] Melikasadat Emami et al. ‘Generalization error of generalized linear models in high dimensions’. In: *International Conference on Machine Learning*. PMLR. 2020.
- [17] Yarin Gal and Zoubin Ghahramani. ‘Dropout as a Bayesian Approximation: Representing Model Uncertainty in Deep Learning’. In: *Proceedings of The 33rd International Conference on Machine Learning*. Ed. by Maria Florina Balcan and Kilian Q. Weinberger. 2016.
- [18] Federica Gerace et al. ‘Generalisation error in learning with random features and the hidden manifold model’. In: *International Conference on Machine Learning*. PMLR. 2020.
- [19] Cédric Gerbelot, Alia Abbara and Florent Krzakala. ‘Asymptotic Errors for High-Dimensional Convex Penalized Linear Regression beyond Gaussian Matrices’. In: *Proceedings of Thirty Third Conference on Learning Theory*. Proceedings of Machine Learning Research. PMLR, 2020.
- [20] Cédric Gerbelot and Raphaël Berthier. ‘Graph-based Approximate Message Passing Iterations’. In: *arXiv:2109.11905 [cs.IT]* (2021).
- [21] Sebastian Goldt et al. ‘Modeling the influence of data structure on learning in neural networks: The hidden manifold model’. In: *Physical Review X* (2020).
- [22] Sebastian Goldt et al. ‘The Gaussian equivalence of generative models for learning with shallow neural networks’. In: *arXiv: 2006.14709 [stat.ML]* (2021).
- [23] Chuan Guo et al. ‘On Calibration of Modern Neural Networks’. In: *Proceedings of the 34th International Conference on Machine Learning* (2017).
- [24] James Hensman, Nicolò Fusi and Neil D. Lawrence. ‘Gaussian Processes for Big Data’. In: *Proceedings of the Twenty-Ninth Conference on Uncertainty in Artificial Intelligence*. UAI’13. Arlington, Virginia, USA: AUAI Press, 2013.
- [25] Yukito Iba. ‘The Nishimori line and Bayesian statistics’. In: *Journal of Physics A: Mathematical and General* (1999).
- [26] Adel Javanmard and Andrea Montanari. ‘State evolution for general approximate message passing algorithms, with applications to spatial coupling’. In: *Information and Inference: A Journal of the IMA* 2.2 (2013).
- [27] Alex Kendall and Yarin Gal. ‘What Uncertainties Do We Need in Bayesian Deep Learning for Computer Vision?’ In: *Proceedings of the 31st International Conference on Neural Information Processing Systems*. NIPS’17. Curran Associates Inc., 2017.
- [28] Balaji Lakshminarayanan, Alexander Pritzel and Charles Blundell. ‘Simple and Scalable Predictive Uncertainty Estimation using Deep Ensembles’. In: *Advances in Neural Information Processing Systems*. Curran Associates, Inc., 2017.
- [29] Jeremiah Zhe Liu et al. ‘Simple and Principled Uncertainty Estimation with Deterministic Deep Learning via Distance Awareness’. In: *Advances in Neural Information Processing Systems* (2020).
- [30] Bruno Loureiro et al. ‘Learning curves of generic features maps for realistic datasets with a teacher-student model’. In: *arXiv: 2102.08127 [stat.ML]* (2021).
- [31] Bruno Loureiro et al. ‘Learning Gaussian Mixtures with Generalised Linear Models: Precise Asymptotics in High-dimensions’. In: *arXiv:2106.03791 [stat.ML]* (2021).

[32] Xiaoyi Mai, Zhenyu Liao and Romain Couillet. ‘A Large Scale Analysis of Logistic Regression: Asymptotic Performance and New Insights’. In: *ICASSP 2019 - 2019 IEEE International Conference on Acoustics, Speech and Signal Processing (ICASSP)*. 2019.

[33] Andrey Malinin, Bruno Mlobozeniec and Mark Gales. ‘Ensemble Distribution Distillation’. In: *International Conference on Learning Representations* (2020).

[34] Song Mei and Andrea Montanari. ‘The Generalization Error of Random Features Regression: Precise Asymptotics and the Double Descent Curve’. In: *Communications on Pure and Applied Mathematics* (2019).

[35] Marc Mezard and Andrea Montanari. *Information, physics, and computation*. Oxford University Press, 2009.

[36] Marc Mézard, Giorgio Parisi and Miguel Angel Virasoro. *Spin glass theory and beyond: An Introduction to the Replica Method and Its Applications*. Vol. 9. World Scientific Publishing Company, 1987.

[37] Francesca Mignacco et al. ‘The Role of Regularization in Classification of High-dimensional Noisy Gaussian Mixture’. In: *Proceedings of the 37th International Conference on Machine Learning*. Proceedings of Machine Learning Research. PMLR, 2020.

[38] Andrea Montanari et al. ‘The generalization error of max-margin linear classifiers: High-dimensional asymptotics in the overparametrized regime’. In: *arXiv:1911.01544 [math.ST]* (2020).

[39] Jishnu Mukhoti et al. ‘Calibrating Deep Neural Networks using Focal Loss’. In: *Advances in Neural Information Processing Systems* (2020).

[40] John Platt. ‘Probabilistic Outputs for Support Vector Machines and Comparisons to Regularized Likelihood Methods’. In: *Adv. Large Margin Classif.* 10 (2000).

[41] Konstantin Posch, Jan Steinbrener and Jürgen Pilz. ‘Variational Inference to Measure Model Uncertainty in Deep Neural Networks’. In: *arXiv:1902.10189 [stat.ML]* (2019).

[42] Sundeep Rangan. ‘Generalized approximate message passing for estimation with random linear mixing’. In: *2011 IEEE International Symposium on Information Theory Proceedings*. IEEE. 2011.

[43] Mohamed El Amine Seddik et al. ‘Random matrix theory proves that deep learning representations of gan-data behave as gaussian mixtures’. In: *International Conference on Machine Learning*. PMLR. 2020, pp. 8573–8582.

[44] Matthias Seeger. ‘Gaussian processes for machine learning’. In: *International journal of neural systems* 02 (2004).

[45] Pragya Sur and Emmanuel J. Candès. ‘A modern maximum-likelihood theory for high-dimensional logistic regression’. In: *Proceedings of the National Academy of Sciences* 116.29 (2019).

[46] Hossein Taheri, Ramtin Pedarsani and Christos Thrampoulidis. ‘Sharp Asymptotics and Optimal Performance for Inference in Binary Models’. In: *Proceedings of the Twenty Third International Conference on Artificial Intelligence and Statistics*. Proceedings of Machine Learning Research. PMLR, 2020.

[47] Christos Thrampoulidis, Ehsan Abbasi and Babak Hassibi. ‘Precise error analysis of regularized M-estimators in high dimensions’. In: *IEEE Transactions on Information Theory* 8 (2018).

[48] Sunil Thulasidasan et al. ‘On Mixup Training: Improved Calibration and Predictive Uncertainty for Deep Neural Networks’. In: *Advances in Neural Information Processing Systems* (2019).

[49] Bianca Zadrozny and Charles Elkan. ‘Obtaining Calibrated Probability Estimates from Decision Trees and Naive Bayesian Classifiers’. In: *ICML* (2001).

[50] Bianca Zadrozny and Charles Elkan. ‘Transforming Classifier Scores into Accurate Multiclass Probability Estimates’. In: *Proceedings of the ACM SIGKDD International Conference on Knowledge Discovery and Data Mining* (2002).

[51] Lenka Zdeborová and Florent Krzakala. ‘Statistical physics of inference: Thresholds and algorithms’. In: *Advances in Physics* (2016).

A Cavity approach to the main results

In this appendix we sketch how the self-consistent equations (16), (18) and (17) characterizing the sufficient statistics $(q_{\text{bo}}, m, q_{\text{erm}})$ can actually be derived via the heuristic cavity method [36, 35] from statistical physics.

We shall use the notation of Rangan's GAMP algorithm [42] and present our results as a derivation of GAMP algorithm from cavity, or belief propagation, as in [51]. This allows to connect all our results as well as the state evolution equations of the GAMP 3.1 algorithm in a single framework. Note that in its most general form, GAMP can be used both as an algorithm for estimating the marginals of the posterior distribution $\mathbf{w}_{\text{amp}} = \mathbb{E}[w|\mathcal{D}]$ or to minimize the empirical risk in 3 - the only difference between the two being the choice of denoising functions (f_{out}, f_w) .

The novelty of our approach consists of running two GAMP algorithms in parallel *on the same instance* of data $\mathcal{D} = \{(\mathbf{x}^\mu, y^\mu)\}_{\mu=1}^n$ drawn from the probit model introduced in eq. (1). Although we run the two versions of GAMP independently, they are correlated through the data \mathcal{D} - and our goal is to characterize exactly their joint distribution.

A.1 Joint state evolution

Consider we are running two AMPs in parallel, one for BO estimation and one for ERM. To distinguish both messages, we will denote ERM messages with a tilde: $\tilde{\omega}^t, \tilde{V}^t$, etc. To derive the asymptotic distribution of the estimators $(\hat{\mathbf{w}}_{\text{amp}}, \hat{\mathbf{w}}_{\text{erm}})$, it is more convenient to start from a close cousin of AMP: the reduced Belief Propagation equations (rBP). Note that in the high-dimensional limit that we are interested in this manuscript, rBP is equivalent to AMP, see for instance [4] or [5] for a detailed derivation. Written in coordinates, the rBP equations are given by:

$$\begin{cases} \omega_{\mu \rightarrow i}^t = \sum_{j \neq i} x_j^\mu \hat{w}_{j \rightarrow \mu}^t \\ V_{\mu \rightarrow i}^t = \sum_{j \neq i} (x_j^\mu)^2 \hat{c}_{j \rightarrow \mu}^t \end{cases}, \quad \begin{cases} g_{\mu \rightarrow i}^t = f_{\text{out}}(y^\mu, \omega_{\mu \rightarrow i}^t, V_{\mu \rightarrow i}^t) \\ \partial g_{\mu \rightarrow i}^t = \partial_\omega f_{\text{out}}(y^\mu, \omega_{\mu \rightarrow i}^t, V_{\mu \rightarrow i}^t) \end{cases} \quad (28)$$

$$\begin{cases} b_{\mu \rightarrow i}^t = \sum_{\nu \neq \mu} x_i^\nu g_{\nu \rightarrow i}^t \\ A_{\mu \rightarrow i}^t = - \sum_{\nu \neq \mu} (x_i^\nu)^2 \partial g_{\nu \rightarrow i}^t \end{cases}, \quad \begin{cases} \hat{w}_{i \rightarrow \mu}^{t+1} f_w(b_{i \rightarrow \mu}^t, A_{i \rightarrow \mu}^t) \\ \hat{c}_{i \rightarrow \mu}^{t+1} \partial_b f_w(b_{\mu \rightarrow i}^t, A_{\mu \rightarrow i}^t) \end{cases} \quad (29)$$

where (f_{out}, f_w) denote the denoising functions that could be associated either to BO or ERM estimation, and that can be generically written in terms of an estimation likelihood P_{out} and prior P_w as:

$$\begin{cases} f_{\text{out}}(y, \omega, V) = \partial_\omega \log \mathcal{Z}_{\text{out}}(y, \omega, V) \\ \mathcal{Z}_{\text{out}}(y, \omega, V) = \int_{\mathbb{R}} \frac{dx}{\sqrt{2\pi V}} e^{-\frac{(x-\omega)^2}{2V}} P_{\text{out}}(y|x) \end{cases}, \quad \begin{cases} f_w(b, A) = \partial_b \log \mathcal{Z}_w(b, A) \\ \mathcal{Z}_w(b, A) = \int_{\mathbb{R}} dw P_w(w) e^{-\frac{1}{2}Aw^2 + bw} \end{cases}. \quad (30)$$

By assumption, the rBP messages are independent from each other, and since we are running both BO and ERM independently, they are only coupled to each other through the data, which has been generated by the same data model:

$$y^\mu \sim P_0(\cdot | \mathbf{w}_\star^\top \mathbf{x}^\mu), \quad \mathbf{x}^\mu \sim \mathcal{N}(0, 1/d \mathbf{I}_d), \quad \mathbf{w}_\star \sim \prod_{i=1}^d P_0(w_{\star i}). \quad (31)$$

Note that here we work in a more general setting than the one in the main manuscript (1). Indeed, the derivation presented here work for *any* factorised distribution of teacher weights \mathbf{w}_\star and any likelihood P_0 (of which the probit is a particular case). For convenience, define the so-called *teacher local field*:

$$z_\mu = \sum_{j=1}^d x_j^\mu w_{\star j} \quad (32)$$

Step 1: Asymptotic joint distribution of $(z_\mu, \omega_{\mu \rightarrow i}^t, \tilde{\omega}_{\mu \rightarrow i}^t)$

Note that $(z_\mu, \omega_{\mu \rightarrow i}^t, \tilde{\omega}_{\mu \rightarrow i}^t)$ are given by a sum of independent random variables with variance $d^{-1/2}$, and therefore by the Central Limit Theorem in the limit $d \rightarrow \infty$ they are asymptotically Gaussian. Therefore we only need to compute their means, variances and cross correlation. The means are straightforward, since x_i^μ have mean zero and therefore they will also have mean zero. The variances are given by:

$$\begin{aligned} \mathbb{E}[z_\mu^2] &= \mathbb{E}\left[\sum_{i=1}^d \sum_{j=1}^d x_i^\mu x_j^\mu w_{\star i} w_{\star j}\right] = \sum_{i=1}^d \sum_{j=1}^d \mathbb{E}[x_i^\mu x_j^\mu] w_{\star i} w_{\star j} = \frac{1}{d} \sum_{i=1}^d \sum_{j=1}^d \delta_{ij} w_{\star i} w_{\star j} \\ &= \frac{\|\mathbf{w}_\star\|_2^2}{d} \xrightarrow{d \rightarrow \infty} \rho \end{aligned} \quad (33)$$

$$\begin{aligned} \mathbb{E}[(\omega_{\mu \rightarrow i}^t)^2] &= \mathbb{E}\left[\sum_{j \neq i}^d \sum_{k \neq i}^d x_j^\mu x_k^\mu \hat{w}_{j \rightarrow \mu}^t \hat{w}_{k \rightarrow \mu}^t\right] = \sum_{j \neq i}^d \sum_{k \neq i}^d \mathbb{E}[x_j^\mu x_k^\mu] \hat{w}_{j \rightarrow \mu}^t \hat{w}_{k \rightarrow \mu}^t = \frac{1}{d} \sum_{j \neq i}^d \sum_{k \neq i}^d \delta_{jk} \hat{w}_{j \rightarrow \mu}^t \hat{w}_{k \rightarrow \mu}^t \\ &= \frac{1}{d} \sum_{j \neq i}^d (\hat{w}_{j \rightarrow \mu}^t)^2 = \frac{\|\hat{\mathbf{w}}^t\|_2^2}{d} - \frac{1}{d} (\hat{w}_{i \rightarrow \mu}^t)^2 \xrightarrow{d \rightarrow \infty} q^t \end{aligned} \quad (34)$$

$$\begin{aligned} \mathbb{E}[z_\mu \omega_{\mu \rightarrow i}^t] &= \mathbb{E}\left[\sum_{j \neq i}^d \sum_{k=1}^d x_j^\mu x_k^\mu \hat{w}_{j \rightarrow \mu}^t w_{\star k}\right] = \sum_{j \neq i}^d \sum_{k=1}^d \mathbb{E}[x_j^\mu x_k^\mu] \hat{w}_{j \rightarrow \mu}^t w_{\star k} = \frac{1}{d} \sum_{j \neq i}^d \sum_{k=1}^d \delta_{jk} \hat{w}_{j \rightarrow \mu}^t w_{\star k} \\ &= \frac{1}{d} \sum_{j \neq i}^d \hat{w}_{j \rightarrow \mu}^t w_{\star j} = \frac{\hat{\mathbf{w}}^t \cdot \mathbf{w}_\star}{d} - \frac{1}{d} \hat{w}_{i \rightarrow \mu}^t w_{\star i} \xrightarrow{d \rightarrow \infty} m^t \end{aligned} \quad (35)$$

$$\begin{aligned} \mathbb{E}[\omega_{\mu \rightarrow i}^t \tilde{\omega}_{\mu \rightarrow i}^t] &= \mathbb{E}\left[\sum_{j \neq i}^d \sum_{k \neq i}^d x_j^\mu x_k^\mu \hat{w}_{j \rightarrow \mu}^t \tilde{w}_{k \rightarrow \mu}^t\right] = \sum_{j \neq i}^d \sum_{k \neq i}^d \mathbb{E}[x_j^\mu x_k^\mu] \hat{w}_{j \rightarrow \mu}^t \tilde{w}_{k \rightarrow \mu}^t = \frac{1}{d} \sum_{j \neq i}^d \sum_{k \neq i}^d \delta_{jk} \hat{w}_{j \rightarrow \mu}^t \tilde{w}_{k \rightarrow \mu}^t \\ &= \frac{1}{d} \sum_{j \neq i}^d \hat{w}_{j \rightarrow \mu}^t \tilde{w}_{j \rightarrow \mu}^t = \frac{\hat{\mathbf{w}}^t \cdot \tilde{\mathbf{w}}^t}{d} - \frac{1}{d} \hat{w}_{i \rightarrow \mu}^t \tilde{w}_{i \rightarrow \mu}^t \xrightarrow{d \rightarrow \infty} Q^t \end{aligned} \quad (36)$$

where we have used that $\hat{w}_{i \rightarrow \mu}^t = O(d^{-1/2})$ to simplify the sums at large d . Summarising our findings:

$$(z_\mu, \omega_{\mu \rightarrow i}^t, \tilde{\omega}_{\mu \rightarrow i}^t) \sim \mathcal{N}\left(\mathbf{0}_3, \begin{bmatrix} \rho & m^t & \tilde{m}^t \\ m^t & q^t & Q^t \\ \tilde{m}^t & Q^t & \tilde{q}^t \end{bmatrix}\right) \quad (37)$$

with:

$$\begin{aligned} \rho &\equiv \frac{1}{d} \|\mathbf{w}_\star\|^2, & q^t &\equiv \frac{1}{d} \|\hat{\mathbf{w}}_{\text{BO}}^t\|^2, & \tilde{q}^t &\equiv \frac{1}{d} \|\hat{\mathbf{w}}_{\text{ERM}}^t\|^2 \\ m^t &\equiv \frac{1}{d} \hat{\mathbf{w}}_{\text{BO}}^t \cdot \mathbf{w}_\star, & \tilde{m}^t &\equiv \frac{1}{d} \hat{\mathbf{w}}_{\text{ERM}}^t \cdot \mathbf{w}_\star, & Q^t &\equiv \frac{1}{d} \hat{\mathbf{w}}_{\text{BO}}^t \cdot \hat{\mathbf{w}}_{\text{ERM}}^t \end{aligned} \quad (38)$$

Step 2: Concentration of variances $V_{\mu \rightarrow i}^t, \tilde{V}_{\mu \rightarrow i}^t$

Since the variances $V_{\mu \rightarrow i}^t, \tilde{V}_{\mu \rightarrow i}^t$ depend on $(x_i^\mu)^2$, in the asymptotic limit $d \rightarrow \infty$ they concentrate around their means:

$$\mathbb{E}[V_{\mu \rightarrow i}^t] = \sum_{j \neq i}^d \mathbb{E}[(x_j^\mu)^2] \hat{c}_{j \rightarrow \mu}^t = \frac{1}{d} \sum_{j \neq i}^d \hat{c}_{j \rightarrow \mu}^t = \frac{1}{d} \sum_{j=1}^d \hat{c}_{j \rightarrow \mu}^t - \frac{1}{d} \hat{c}_{i \rightarrow \mu}^t \xrightarrow{d \rightarrow \infty} V^t \equiv \frac{1}{d} \sum_{j=1}^d \hat{c}_j^t \quad (39)$$

where we have defined the variance overlap V^t . The same argument can be used for $\tilde{V}_{\mu \rightarrow i}^t$. Summarising, asymptotically we have:

$$V_{\mu \rightarrow i}^t \rightarrow V^t, \quad \tilde{V}_{\mu \rightarrow i}^t \rightarrow \tilde{V}^t \quad (40)$$

Step 3: Distribution of $b_{\mu \rightarrow i}^t, \tilde{b}_{\mu \rightarrow i}^t$

By definition, we have

$$b_{\mu \rightarrow i}^t = \sum_{\nu \neq \mu} x_i^\nu g_{\nu \rightarrow i}^t = \sum_{\nu \neq \mu} x_i^\nu f_{\text{out}}(y^\mu, \omega_{\nu \rightarrow i}^t, V_{\nu \rightarrow i}^t) = \sum_{\nu \neq \mu} x_i^\nu f_{\text{out}}(f_0(z_\nu + \tau \xi_\nu), \omega_{\nu \rightarrow i}^t, V_{\nu \rightarrow i}^t) \quad (41)$$

Note that in the sum $z_\nu = \sum_{j=1}^d x_j^\nu w_{\star j}$ there is a term $i = j$, and therefore z_μ is correlated with x_i^ν . To make this explicit, we split the teacher local field:

$$z_\mu = \sum_{j=1}^d x_j^\mu w_{\star j} = \underbrace{\sum_{j \neq i} x_j^\mu w_{\star j}}_{z_{\mu \rightarrow i}} + x_i^\mu w_{\star i} \quad (42)$$

and note that $z_{\mu \rightarrow i} = O(1)$ is independent from x_i^ν . Since $x_i^\mu w_{\star i} = O(d^{-1/2})$, to take the average at leading order, we can expand the denoising function:

$$f_{\text{out}}(f_0(z_\mu + \tau \xi_\mu), \omega_{\nu \rightarrow i}^t, V_{\nu \rightarrow i}^t) = f_{\text{out}}(f_0(z_{\nu \rightarrow i} + \tau \xi_\nu), \omega_{\nu \rightarrow i}^t, V_{\nu \rightarrow i}^t) + \partial_z f_{\text{out}}(f_0(z_{\nu \rightarrow i} + \tau \xi_\nu), \omega_{\nu \rightarrow i}^t, V_{\nu \rightarrow i}^t) x_i^\nu w_{\star i} + O(d^{-3/2})$$

Inserting in the expression for $b_{\mu \rightarrow i}^t$,

$$b_{\mu \rightarrow i}^t = \sum_{\nu \neq \mu} x_i^\nu f_{\text{out}}(f_0(z_{\nu \rightarrow i} + \tau \xi_\nu), \omega_{\nu \rightarrow i}^t, V_{\nu \rightarrow i}^t) + \sum_{\nu \neq \mu} (x_i^\nu)^2 \partial_z f_{\text{out}}(f_0(z_{\nu \rightarrow i} + \tau \xi_\nu), \omega_{\nu \rightarrow i}^t, V_{\nu \rightarrow i}^t) w_{\star i} + O(d^{-3/2})$$

Therefore:

$$\begin{aligned} \mathbb{E}[b_{\mu \rightarrow i}^t] &= \frac{w_{\star i}}{d} \sum_{\nu \neq \mu} \partial_z f_{\text{out}}(f_0(z_{\nu \rightarrow i} + \tau \xi_\nu), \omega_{\nu \rightarrow i}^t, V_{\nu \rightarrow i}^t) + O(d^{-3/2}) \\ &= \frac{w_{\star i}}{d} \sum_{\nu=1}^n \partial_z f_{\text{out}}(f_0(z_{\nu \rightarrow i} + \tau \xi_\nu), \omega_{\nu \rightarrow i}^t, V_{\nu \rightarrow i}^t) + O(d^{-3/2}) \end{aligned} \quad (43)$$

Note that as $d \rightarrow \infty$, for fixed t and for all ν , the fields $(z_{\nu \rightarrow i}, \omega_{\nu \rightarrow i}^t)$ are identically distributed according to average in eq. (37). Therefore,

$$\frac{1}{d} \sum_{\nu=1}^n \partial_z f_{\text{out}}(f_0(z_{\nu \rightarrow i} + \tau \xi_\nu), \omega_{\nu \rightarrow i}^t, V_{\nu \rightarrow i}^t) \xrightarrow{d \rightarrow \infty} \alpha \mathbb{E}_{(\omega, z), \xi} [\partial_z f_{\text{out}}(f_0(z + \tau \xi), \omega, V^t)] \equiv \hat{m}^t \quad (44)$$

so:

$$\mathbb{E}[b_{\mu \rightarrow i}^t] \xrightarrow{d \rightarrow \infty} w_{\star i} \hat{m}^t. \quad (45)$$

Similarly, the variance is given by:

$$\begin{aligned} \text{Var}[b_{\mu \rightarrow i}^t] &= \sum_{\nu \neq \mu} \sum_{\kappa \neq \mu} \mathbb{E}[x_i^\nu x_i^\kappa] f_{\text{out}}(f_0(z_{\nu \rightarrow i} + \tau \xi_\nu), \omega_{\nu \rightarrow i}^t, V_{\nu \rightarrow i}^t) f_{\text{out}}(f_0(z_{\kappa \rightarrow i} + \tau \xi_\kappa), \omega_{\kappa \rightarrow i}^t, V_{\kappa \rightarrow i}^t) + O(d^{-2}) \\ &= \frac{1}{d} \sum_{\nu \neq \mu} f_{\text{out}}(f_0(z_{\nu \rightarrow i} + \tau \xi_\nu), \omega_{\nu \rightarrow i}^t, V_{\nu \rightarrow i}^t)^2 + O(d^{-2}) \\ &= \frac{1}{d} \sum_{\nu=1}^n f_{\text{out}}(f_0(z_{\nu \rightarrow i} + \tau \xi_\nu), \omega_{\nu \rightarrow i}^t, V_{\nu \rightarrow i}^t)^2 + O(d^{-2}) \\ &\xrightarrow{d \rightarrow \infty} \alpha \mathbb{E}_{(z, \omega), \xi} [f_{\text{out}}(f_0(z + \tau \xi), \omega, V^t)^2] \equiv \hat{q}^t \end{aligned} \quad (46)$$

The same discussion holds for the ERM. We now just need to compute the correlation between both fields:

$$\begin{aligned} \text{Cov} \left[b_{\mu \rightarrow i}^t, \tilde{b}_{\mu \rightarrow i}^t \right] &= \sum_{\nu \neq \mu} \sum_{\kappa \neq \mu} \mathbb{E} [x_i^\nu x_i^\kappa] f_{\text{out}}(f_0(z_{\nu \rightarrow i} + \tau \xi_\nu), \omega_{\nu \rightarrow i}^t, V_{\nu \rightarrow i}^t) \tilde{f}_{\text{out}}(f_0(z_{\kappa \rightarrow i} + \tau \xi_\kappa), \tilde{\omega}_{\kappa \rightarrow i}^t, \tilde{V}_{\kappa \rightarrow i}^t) + O(d^{-2}) \\ &= \frac{1}{d} \sum_{\nu=1}^n f_{\text{out}}(f_0(z_{\nu \rightarrow i} + \tau \xi_\nu), \omega_{\nu \rightarrow i}^t, V_{\nu \rightarrow i}^t) \tilde{f}_{\text{out}}(f_0(z_{\nu \rightarrow i} + \tau \xi_\nu), \tilde{\omega}_{\nu \rightarrow i}^t, \tilde{V}_{\nu \rightarrow i}^t) + O(d^{-2}) \\ &\xrightarrow[d \rightarrow \infty]{} \alpha \mathbb{E}_{(z, \omega, \tilde{\omega}), \xi} \left[f_{\text{out}}(f_0(z + \tau \xi), \omega, V^t) \tilde{f}_{\text{out}}(f_0(z + \tau \xi), \tilde{\omega}, \tilde{V}^t) \right] \equiv \hat{Q}^t \end{aligned} \quad (47)$$

To summarise, we have:

$$(b_{\mu \rightarrow i}^t, \tilde{b}_{\mu \rightarrow i}^t) \sim \mathcal{N} \left(w_{\star i} \begin{bmatrix} \hat{m}^t \\ \tilde{\hat{m}}^t \end{bmatrix}, \begin{bmatrix} \hat{q}^t & \hat{Q}^t \\ \hat{Q}^t & \tilde{\hat{q}}^t \end{bmatrix} \right) \quad (48)$$

Step 4: Concentration of $A_{\mu \rightarrow i}^t, \tilde{A}_{\mu \rightarrow i}^t$

The only missing piece is to determine the distribution of the prior variances $A_{\mu \rightarrow i}^t, \tilde{A}_{\mu \rightarrow i}^t$. Similar to the previous variance, they concentrate:

$$\begin{aligned} A_{\mu \rightarrow i}^t &= - \sum_{\nu \neq \mu} (x_i^\nu)^2 \partial_\omega f_{\text{out}}(y^\nu, \omega_{\nu \rightarrow i}^t, V_{\nu \rightarrow i}^t) = - \sum_{\nu \neq \mu} (x_i^\nu)^2 \partial_\omega f_{\text{out}}(f_0(z_{\nu \rightarrow i} + \tau \xi_\nu), \omega_{\nu \rightarrow i}^t, V_{\nu \rightarrow i}^t) + O(d^{-3/2}) \\ &= - \frac{1}{d} \sum_{\nu=1}^n \partial_\omega f_{\text{out}}(f_0(z_{\nu \rightarrow i} + \tau \xi_\nu), \omega_{\nu \rightarrow i}^t, V_{\nu \rightarrow i}^t) + O(d^{-3/2}) \\ &\xrightarrow[d \rightarrow \infty]{} -\alpha \mathbb{E}_{(z, \omega), \xi} [\partial_\omega f_{\text{out}}(f_0(z + \tau \xi), \omega, V^t)] \equiv \hat{V}^t \end{aligned} \quad (49)$$

Summary

We now have all the ingredients we need to characterise the asymptotic distribution of the estimators:

$$\hat{\mathbf{w}}_{\text{BO}} \sim f_{\text{out}}(\mathbf{w}_\star \hat{m}^t + \sqrt{\hat{q}^t} \xi, \hat{V}^t) \quad (50)$$

$$\hat{\mathbf{w}}_{\text{ERM}} \sim \tilde{f}_{\text{out}}(\mathbf{w}_\star \tilde{\hat{m}}^t + \sqrt{\tilde{\hat{q}}^t} \eta, \tilde{V}^t) \quad (51)$$

where $\eta, \xi \sim \mathcal{N}(\mathbf{0}, \mathbf{I}_d)$ are independent Gaussian variables. From that, we can recover the usual GAMP state evolution equations for the overlaps:

$$\begin{cases} V^{t+1} = \mathbb{E}_{(w_\star, \xi)} \left[\partial_b f_w(\hat{m}^t w_\star + \sqrt{\hat{q}^t} \xi, \hat{V}^t) \right] \\ q^{t+1} = \mathbb{E}_{(w_\star, \xi)} \left[f_w(\hat{m}^t w_\star + \sqrt{\hat{q}^t} \xi, \hat{V}^t)^2 \right] \\ m^{t+1} = \mathbb{E}_{(w_\star, \xi)} \left[f_w(\hat{m}^t w_\star + \sqrt{\hat{q}^t} \xi, \hat{V}^t) w_{\star i} \right] \end{cases}, \quad \begin{cases} \hat{V}^t = -\alpha \mathbb{E}_{(z, \omega), \xi} [\partial_\omega f_{\text{out}}(f_0(z + \tau \xi), \omega, V^t)] \\ \hat{q}^t = \alpha \mathbb{E}_{(z, \omega), \xi} [f_{\text{out}}(f_0(z + \tau \xi), \omega, V^t)^2] \\ \hat{m}^t = \alpha \mathbb{E}_{(z, \omega), \xi} [f_{\text{out}}(f_0(z + \tau \xi), \omega, V^t)] \end{cases} \quad (52)$$

which is also valid for the tilde variables. But we can also get a set of equations for the correlations:

$$\begin{cases} Q^t = \mathbb{E}_{w_\star, (b, \tilde{b})} \left[f_w(b, \hat{V}^t) \tilde{f}_w(\tilde{b}, \tilde{V}^t) \right] \\ \hat{Q}^t = \alpha \mathbb{E}_{(z, \omega, \tilde{\omega}), \xi} \left[f_{\text{out}}(f_0(z + \tau \xi), \omega, V^t) \tilde{f}_{\text{out}}(f_0(z + \tau \xi), \tilde{\omega}, \tilde{V}^t) \right] \end{cases} \quad (53)$$

A.2 Simplifications

Simplifying BO state evolution

State evolution of BO can be reduced to two equations. First, note that asymptotically

$$m := \frac{1}{d} \hat{\mathbf{w}}_{\text{bo}} \cdot \mathbf{w}_\star = \frac{1}{d} \mathbb{E}_{\mathbf{w}_\star, \mathcal{D}} [\hat{\mathbf{w}}_{\text{bo}} \cdot \mathbf{w}_\star]$$

with high probability. By Nishimori identity, the vector \mathbf{w}_* in the expectation can be replaced by an independent copy of the Bayesian posterior. This yields :

$$\frac{1}{d} \mathbb{E}_{\mathbf{w}_*, \mathcal{D}} [\hat{\mathbf{w}}_{\text{bo}} \cdot \mathbf{w}_*] = \frac{1}{d} \mathbb{E}_{\mathcal{D}} [\hat{\mathbf{w}}_{\text{bo}}] = q$$

Hence $m = q$. Similarly, noting $\langle \cdot \rangle$ the average over the posterior distribution :

$$V = \frac{1}{d} \langle \|\mathbf{w} - \hat{\mathbf{w}}_{\text{bo}}\|^2 \rangle = \frac{1}{d} \mathbb{E}_{\mathcal{D}} [\langle \|\mathbf{w} - \hat{\mathbf{w}}_{\text{bo}}\|^2 \rangle] = \frac{1}{d} \mathbb{E}_{\mathcal{D}} [\langle \|\mathbf{w}\|^2 \rangle] - \frac{1}{d} \mathbb{E}_{\mathcal{D}} [\hat{\mathbf{w}}_{\text{bo}} \cdot \hat{\mathbf{w}}_{\text{bo}}]$$

Like before, we used the fact that in asymptotically, $\langle \|\mathbf{w} - \hat{\mathbf{w}}_{\text{bo}}\|^2 \rangle$ concentrates around its mean. Using Nishimori, the first term is equal to $\mathbb{E}_{\mathbf{w}_*} [\|\mathbf{w}_*\|^2] = 1$. By definition, the second term is equal to q , thus $V = 1 - q$.

Using similar arguments, $\hat{m} = \hat{q} = \hat{V}$. Thus, the state evolution can be reduced to two equations on q and \hat{q} .

Simplifying the Q, \hat{Q} equations

In fact, the Nishimori property also allow us to show that the cross-correlation Q, \hat{Q} are the same as the overlaps $\tilde{m}, \hat{\tilde{m}}$, in a similar way to [A.2](#). Indeed,

$$Q = \frac{1}{d} \hat{\mathbf{w}}_{\text{bo}} \cdot \hat{\mathbf{w}}_{\text{erm}} = \frac{1}{d} \mathbb{E}_{\mathcal{D}} [\hat{\mathbf{w}}_{\text{bo}} \cdot \hat{\mathbf{w}}_{\text{erm}}] = \frac{1}{d} \mathbb{E}_{\mathbf{w}_*, \mathcal{D}} [\mathbf{w}_* \cdot \hat{\mathbf{w}}_{\text{erm}}] = \tilde{m} \quad (54)$$

Alternatively, we can also prove that directly showing that the iterations for Q^t are a stable orbit of \tilde{m}^t . Indeed, assume that at time step t we have $Q^t = \tilde{m}^t$ and $\hat{Q}^t = \hat{\tilde{m}}^t$. Then, focusing at our specific setting, at time $t + 1$ we have:

$$\begin{aligned} Q^{t+1} &= \mathbb{E}_{\mathbf{w}_*, b, \tilde{b}} [f_w(b, \hat{V}) f_w(b, \hat{V})] = \mathbb{E}_{\mathbf{w}_*} \left[\frac{b}{\hat{V} + 1} \frac{\tilde{b}}{\hat{V} + \lambda} \right] = \mathbb{E}_{\mathbf{w}_*} \left[\frac{\hat{Q} + \hat{\tilde{m}} \hat{m}}{(\hat{V} + 1)(\hat{V} + \lambda)} \right] \\ &= \mathbb{E}_{\mathbf{w}_*} \left[\frac{\hat{\tilde{m}}}{\hat{V} + \lambda} \right]. \end{aligned}$$

Because as we have shown above $\hat{m} = \hat{q}$ and $\hat{Q}^t = \hat{\tilde{m}}^t$. This is precisely the equation for \tilde{m} .

A.3 Evaluating the equations

Bayes-optimal

In Bayes-optimal estimation, the estimation likelihood P_{out} and prior P_w match exactly that of the generating model for data, which for the model (1) is:

$$P_{\text{out}}(y|x) = \frac{1}{2} \text{erfc} \left(-\frac{y\omega}{\sqrt{2\Delta}} \right), \quad P_w(w) = \mathcal{N}(0, 1). \quad (55)$$

Therefore, it is easy to show that:

$$\mathcal{Z}_{\text{out}}(y, \omega, V) = \frac{1}{2} \text{erfc} \left(-\frac{y\omega}{\sqrt{2(\tau^2 + V)}} \right), \quad Z_w(b, A) = \frac{e^{\frac{b^2}{1+A}}}{1+A} \quad (56)$$

and therefore:

$$f_{\text{out}}(y, \omega, V) = \frac{2y \mathcal{N}(\omega y | 0, V + \tau^2)}{\text{erfc} \left(-\frac{y\omega}{\sqrt{2(\tau^2 + V)}} \right)}, \quad f_w(b, A) = \frac{b}{1+A} \quad (57)$$

This form of the prior allow us to simplify some of the equations considerably:

$$q_{\text{bo}}^{t+1} = \mathbb{E}_{(w_\star, \xi)} \left[f_w(\hat{q}^t w_\star + \sqrt{\hat{q}^t} \xi, \hat{q}^t)^2 \right] = \frac{1}{1 + \hat{q}_{\text{bo}}^t} \quad (58)$$

which is the equation found in Theorem 3.2. The other equation cannot be closed analytically, however it can be considerably simplified:

$$\hat{q}_{\text{bo}} = -\alpha \mathbb{E}_{(z, \omega), \xi} [\partial_\omega f_{\text{out}}(f_0(z + \tau \xi), \omega, V^t)] \quad (59)$$

$$= \frac{2}{\pi} \frac{\alpha}{1 + \tau^2 - q_{\text{bo}}^t} \int_{\mathbb{R}} dz \mathcal{N} \left(z \middle| 0, \frac{q_{\text{bo}}^t}{2(1 + \tau^2 - q_{\text{bo}}^t)} \right) \frac{e^{-2z^2}}{\text{erfc}(z)\text{erfc}(-z)} \quad (60)$$

A.4 ERM estimation

For ERM, the estimation likelihood P_{out} and prior P_w are related to the loss and penalty functions:

$$P_{\text{out}}(y|x) = e^{-\beta \ell(y, x)}, \quad P_w(w) = e^{-\beta r(w)}. \quad (61)$$

where the parameter $\beta > 0$ is introduced for convenience, and should be taken to infinity. Focusing on the regularisation part and redefining $(b, A) \rightarrow (\beta b, \beta A)$

$$\mathcal{Z}_w(b, A) = \int_{\mathbb{R}} dw e^{-\beta \left(\frac{A}{2} w^2 - bw + r(w) \right)} \underset{\beta \rightarrow \infty}{\asymp} e^{\beta \left[\frac{b^2}{2A} - \mathcal{M}_{A^{-1}r}(A^{-1}b) \right]} \quad (62)$$

where we have used Laplace's method and defined the *Moreau envelope*:

$$\mathcal{M}_{\tau f}(x) = \min_{z \in \mathbb{R}} \left[\frac{1}{2\tau} (x - z)^2 + f(z) \right] \quad (63)$$

$$(64)$$

Therefore,

$$f_w(b, A) = \lim_{\beta \rightarrow \infty} \frac{1}{\beta} \partial_b \log \mathcal{Z}_w(b, A) = \text{prox}_{A^{-1}r}(A^{-1}b) \quad (65)$$

where we have defined the *proximal operator*:

$$\text{prox}_{\tau f}(x) = \underset{z \in \mathbb{R}}{\text{argmin}} \left[\frac{1}{2\tau} (x - z)^2 + f(z) \right] \quad (66)$$

and used the well-known property $\partial_x \mathcal{M}_{\tau f}(x) = -\frac{1}{\tau} (\text{prox}_{\tau f}(x) - x)$. In particular, for the ℓ_2 -penalty $r(w) = \lambda/2w^2$, we have:

$$\text{prox}_{\lambda/2(\cdot)^2}(x) = \frac{x}{1 + \lambda} \quad \Leftrightarrow \quad f_w(b, A) = \frac{b}{\lambda + A} \quad (67)$$

The simple form of the regularization allow us to simplify the state evolution equations considerably:

$$\begin{cases} \tilde{V}^{t+1} &= \mathbb{E}_{(w_\star, \xi)} \left[\partial_b f_w(\hat{m}^t w_\star + \sqrt{\hat{q}^t} \xi, \hat{V}^t) \right] = \frac{1}{\lambda + \hat{V}} \\ \tilde{q}^{t+1} &= \mathbb{E}_{(w_\star, \xi)} \left[f_w(\hat{m}^t w_\star + \sqrt{\hat{q}^t} \xi, \hat{V}^t)^2 \right] = \frac{\hat{m}^2 + \hat{q}^t}{(\lambda + \hat{V})^2} \\ \tilde{m}^{t+1} &= \mathbb{E}_{(w_\star, \xi)} \left[f_w(\hat{m}^t w_\star + \sqrt{\hat{q}^t} \xi, \hat{V}^t) w_{\star i} \right] = \frac{\hat{m}}{\lambda + \hat{V}} \end{cases} \quad (68)$$

which are the equations found in Theorem 3.2. A similar discussion can be carried for the loss term, and yields in general:

$$f_{\text{out}}(y, \omega, V) = V^{-1} \left(\text{prox}_{\tau \ell(y, \cdot)}(x) - x \right) \quad (69)$$

Unfortunately, the logistic loss $\ell(y, x) = \log(1 + e^{-yx})$ does not admit a closed form solution for the proximal, and therefore for a given (y, ω, V) we need to compute it numerically.

B Proof of main theorems

A possible route for proving our result is to give a rigorous proof of the cavity equations. Instead, we shall use a shortcut, and leverage on recent progresses for both the ERM cavity results [47, 45, 12, 38, 3, 30]), the Bayes performances [8, 9], as well as on the performance of GAMP [42, 26, 20].

B.1 GAMP optimality

The optimality of GAMP is a direct consequence of the generic results concerning its performance (the state evolution in [42, 26]) and the characterization of the Bayes performance in [9]. G-a works, one considers a sequence of inference problems indexed by the dimension d , with data \mathcal{D}_d (which are defined in section 2 for our purpose). As d increases, both GAMP performances and Bayes errors converge with high probability to the same deterministic limit given by the so-called "replica", or "state evolution" equations.

To simplify the notation, all our statements involving the asymptotic limit $d \rightarrow \infty$ are implicitly defined for such sequences, and the convergence is assumed to be in terms of probability.

Let us prove that, indeed, GAMP estimates for posterior probability are asymptotically exact with high probability. First, we note that the estimation of the Bayes posterior probability for the signs corresponds to finding the estimators that minimize the MMSE. Indeed consider, for fixed data (this remains true averaging over data), the mean squared error for an estimator $\hat{Y}(\mathbf{X})$:

$$\text{MSE}(\hat{Y}(\mathbf{X})) = \mathbb{E}_{Y, \mathbf{X}} \left[(Y - \hat{Y}(\mathbf{X}))^2 \right] = \mathbb{E}_{\mathbf{X}} \mathbb{E}_{Y|\mathbf{X}} \left[(Y - \hat{Y}(\mathbf{X}))^2 \right] \quad (70)$$

The mean square error is given by using the posterior mean [13], as can be seen immediately differentiating with respect to \hat{Y} (for a given \mathbf{x}), so that:

$$\hat{Y}_{\text{Bayes}}(\mathbf{x}) = \mathbb{E}_{Y|X=\mathbf{x}}[Y] = 2\mathbb{P}_{Y|X=\mathbf{x}}(Y = 1) - 1 \quad (71)$$

The Bayes estimator for the posterior probability is thus the MMSE estimator. We see here that the estimation of the posterior mean of Y is equivalent to the estimation of the probability it takes value one; both quantities are thus trivially related.

We can now use Proposition 2, page 12 in [9], that shows that indeed GAMP efficiently achieves Bayes-optimality for the MMSE on Y :

Theorem B.1 (GAMP generalisation error, [9]). *Consider a sequence of problems indexed by d , with data \mathcal{D}_d in dimension d , then we have that GAMP estimator asymptotically achieves the Minimal Mean Square Error in estimating the error on new label Y . That is, with high probability:*

$$\lim_{d \rightarrow \infty} \mathbb{E}_{Y, \mathbf{X}|\mathcal{D}_d} \left[(Y - \hat{Y}_{\text{GAMP}}(\mathbf{X}, \mathcal{D}_d))^2 \right] = \text{MMSE}(Y) \quad (72)$$

where $\hat{Y}_{\text{GAMP}}(\mathbf{x}, \mathcal{D}) = 2p - 1$, and $p = \hat{f}^{\text{AMP}}(\mathbf{x})$ (eq. 9), with $\hat{\mathbf{c}}_{\text{amp}}^\top(\mathbf{x} \odot \mathbf{x}) = 1 - q$, with q a fixed point of (16).

The fact that GAMP asymptotically achieves the MMSE, coupled with the uniqueness of the Bayes estimator, implies the GAMP estimator for p is arbitrary close to the Bayes estimated for p , with high probability over new Gaussian samples, as $d \rightarrow \infty$. More precisely, we can use the following lemma:

Lemma B.2 (Bounds on differences of estimators for Y). *Consider a sequence of estimation problems indexed by d with data \mathcal{D}_d . If a (sequence of) estimators $\hat{f}_d(\mathbf{x})$ achieves the MMSE performance of $\hat{g}_d^{\text{Bayes}}(\mathbf{x})$ as $d \rightarrow \infty$ for Gaussian distributed \mathbf{x} , then*

$$\lim_{d \rightarrow \infty} \mathbb{E}_{\mathbf{X}} |f_d(\mathbf{X}) - g_d^{\text{Bayes}}(\mathbf{X})|^2 \rightarrow 0 \quad (73)$$

Proof. The Bayes estimator $g_d^{\text{Bayes}}()$ is the minimum of the MMSE, therefore for any other estimator $f_d(\mathbf{X})$ we have

$$\mathbb{E} [(Y - f_d(\mathbf{X}))^2] \geq \mathbb{E} [(Y - g_d^{\text{Bayes}}(\mathbf{X}))^2]. \quad (74)$$

We have, denoting $\delta_d(X) = f_d(\mathbf{X}) - g_d^{\text{Bayes}}(\mathbf{X})$

$$\mathbb{E} [(Y - f_d(\mathbf{X}))^2] = \mathbb{E} [(Y - g_d^{\text{Bayes}}(\mathbf{X}) + \delta_d(X))^2] \quad (75)$$

$$= \text{MMSE} + \mathbb{E} [\delta_d(X)^2 + 2\delta_n(X)(Y - g_d^{\text{Bayes}}(X))] \quad (76)$$

$$= \text{MMSE} + \mathbb{E} [\delta_d(X)^2] + \mathbb{E}_{X, \mathcal{D}} \mathbb{E}_{Y|X, \mathcal{D}} [2\delta_d(X)(Y - g_d^{\text{Bayes}}(X))] \quad (77)$$

$$= \text{MMSE} + \mathbb{E} [\delta_d(X)^2] + \mathbb{E}_{X, \mathcal{D}} [2\delta_n(X) \mathbb{E}_{Y|X, \mathcal{D}} [Y - g_d^{\text{Bayes}}(X)]] \quad (78)$$

$$= \text{MMSE} + \mathbb{E} [\delta_d(X)^2] \quad (79)$$

where we have used $g_d^{\text{Bayes}}(X) = \mathbb{E}_{Y|X, \mathcal{D}} [Y]$. Using the fact that the f_d asymptotically achieve MMSE optimality, we thus obtain:

$$\lim_{d \rightarrow \infty} \mathbb{E}_{Y, X, \mathcal{D}} [|f_d(X) - g_d^{\text{Bayes}}(X)|^2] \rightarrow 0 \quad (80)$$

□

Applying this lemma to the GAMP estimator leads to Theorem 3.1: with high probability over new sample \mathbf{x} and learning data \mathcal{D} , the GAMP estimate is asymptotically equivalent to the Bayes one.

B.2 Joint density of estimators

While a possible strategy to prove the second theorem would be to use state evolution to follow our joint GAMP algorithm (thus monitoring the Bayes *and* the ERM performance), we shall instead again leverage on recent progresses on generic proofs of replica equations, in particular the Bayes one (in [9] and the ERM ones (that were the subject of many works recently [47, 45, 12, 38, 3, 30]). Again, all our statements involving the asymptotic limit $d \infty$ are implicitly defined for sequences of problems, and the convergence is assumed to be in terms of probability. We start by the following lemma:

Lemma B.3 (Joint distribution of pre-activation). *For a fixed set of data \mathcal{D} , consider the joint random variables (over \mathbf{X}) $\nu = \mathbf{X} \cdot \mathbf{w}_*$, $\lambda_{\text{erm}} = \mathbf{X} \cdot \hat{\mathbf{w}}_{\text{erm}}$, $\lambda_{\text{amp}} = \mathbf{X} \cdot \hat{\mathbf{w}}_{\text{amp}}$. Then we have*

$$\mathbb{P}(\nu, \lambda_{\text{amp}}, \lambda_{\text{erm}}) = \mathcal{N} \left(0, \begin{pmatrix} \frac{\mathbf{w}_* \cdot \mathbf{w}_*}{d} & \frac{\mathbf{w}_* \cdot \hat{\mathbf{w}}_{\text{amp}}}{d} & \frac{\mathbf{w}_* \cdot \hat{\mathbf{w}}_{\text{erm}}}{d} \\ \frac{\hat{\mathbf{w}}_{\text{amp}} \cdot \mathbf{w}_*}{d} & \frac{\hat{\mathbf{w}}_{\text{amp}} \cdot \hat{\mathbf{w}}_{\text{amp}}}{d} & \frac{\hat{\mathbf{w}}_{\text{amp}} \cdot \hat{\mathbf{w}}_{\text{erm}}}{d} \\ \frac{\hat{\mathbf{w}}_{\text{erm}} \cdot \mathbf{w}_*}{d} & \frac{\hat{\mathbf{w}}_{\text{erm}} \cdot \hat{\mathbf{w}}_{\text{amp}}}{d} & \frac{\hat{\mathbf{w}}_{\text{erm}} \cdot \hat{\mathbf{w}}_{\text{erm}}}{d} \end{pmatrix} \right) \quad (81)$$

Proof. This is an immediate consequence of the Gaussianity of the new data \mathbf{x} , with covariance \mathbb{I}/d . □

We now would like to know the asymptotic limit of the parameters of this distribution, for large d . While we have $\frac{\mathbf{w}_* \cdot \mathbf{w}_*}{d} \rightarrow \rho$, the other overlap have a deterministic limit given by the replica equations. For empirical risk minimisation, this has been proven in the aforementioned series of works, but we shall here use the notation of [30] and utilize use the following results:

Theorem B.4 (ERM overlaps [47, 3, 30]). *Consider a sequence of inference problem indexed by the dimension d , then with high probability:*

$$\lim_{d \rightarrow \infty} \frac{\hat{\mathbf{w}}_{\text{erm}} \cdot \mathbf{w}_*}{d} \rightarrow m, \quad \lim_{d \rightarrow \infty} \frac{\hat{\mathbf{w}}_{\text{erm}} \cdot \hat{\mathbf{w}}_{\text{erm}}}{d} \rightarrow q_{\text{erm}} \quad (82)$$

With q_{erm} and m solutions of the self-consistent equations (17) in the main text.

GAMP is tracked by its state evolution [26], and is known to achieve the Bayes overlap:

Theorem B.5 (Bayes overlaps [9]). *Consider a sequence of inference problem indexed by the dimension d , then with high probability:*

$$\lim_{d \rightarrow \infty} \frac{\hat{\mathbf{w}}_{\text{amp}} \cdot \mathbf{w}_*}{d} \rightarrow q_{\text{bo}}, \quad \lim_{d \rightarrow \infty} \frac{\hat{\mathbf{w}}_{\text{amp}} \cdot \hat{\mathbf{w}}_{\text{amp}}}{d} \rightarrow q_{\text{bo}} \quad (83)$$

With q_{bo} given by the self-consistent Equation (16).

The only overlap left to control is thus $Q = \hat{\mathbf{w}}_{\text{amp}} \cdot \hat{\mathbf{w}}_{\text{erm}}/d$. We shall now prove that it is also concentrating, with high probability, to m . To do this, we first prove the following lemma for the overlap between the Bayes estimate $\mathbf{w}_{\text{bo}} = \mathbb{E}_{W|\mathcal{D}}[\mathbf{W}]$ and any other vector \mathbf{V} , possibly dependent on the data:

Lemma B.6 (Nishimori relation for Bayes overlaps).

$$\mathbb{E}_{\mathcal{D}} [\mathbf{w}_{\text{bo}} \cdot \mathbf{V}(\mathcal{D})] = \mathbb{E}_{\mathcal{D}, W^*} [\mathbf{w}^* \cdot \mathbf{V}(\mathcal{D})] \quad (84)$$

Proof. The proof is an application of Bayes formula, and an example of what is often called a Nishimori equality in statistical physics:

$$\mathbb{E}_{\mathcal{D}, W^*} [\mathbf{w}^* \cdot \mathbf{V}(\mathcal{D})] = \mathbb{E}_{\mathcal{D}} \mathbb{E}_{W^*|\mathcal{D}} [\mathbf{w}^* \cdot \mathbf{V}(\mathcal{D})] \quad (85)$$

$$= \mathbb{E}_{\mathcal{D}} [(E_{W^*|\mathcal{D}} \mathbf{w}^*) \cdot \mathbf{V}(\mathcal{D})] = \mathbb{E}_{\mathcal{D}} [\mathbf{w}_{\text{bo}} \cdot \mathbf{V}(\mathcal{D})] \quad (86)$$

□

From this lemma, we see immediately that, in expectation

$$\lim_{d \rightarrow \infty} \mathbb{E} \left[\frac{\mathbf{w}_{\text{erm}} \cdot \mathbf{w}_*}{d} \right] = \lim_{d \rightarrow \infty} \mathbb{E} \left[\frac{\mathbf{w}_{\text{erm}} \cdot \mathbf{w}_{\text{bo}}}{d} \right] = m \quad (87)$$

Additionally, we already know that the left hand side concentrates. It is easy to see that the right hand side does as well:

Lemma B.7 (Concentration of the overlap Q).

$$\lim_{d \rightarrow \infty} \mathbb{E} \left[\left(\frac{\mathbf{w}_{\text{bo}} \cdot \mathbf{w}_{\text{erm}}}{d} \right)^2 \right] = \lim_{d \rightarrow \infty} \mathbb{E} \left[\frac{\mathbf{w}_{\text{bo}} \cdot \mathbf{w}_{\text{erm}}}{d} \right]^2 \quad (88)$$

Proof. The proof again uses Nishimori identity.

$$\mathbb{E} \left[\left(\frac{\mathbf{w}_{\text{bo}} \cdot \mathbf{w}_{\text{erm}}}{d} \right)^2 \right] = \mathbb{E} \left[\left(\frac{\mathbf{w}_{\text{bo}} \cdot \mathbf{w}_{\text{erm}}}{d} \right) \left(\frac{\mathbf{w}_{\text{bo}} \cdot \mathbf{w}_{\text{erm}}}{d} \right) \right] \quad (89)$$

$$= \mathbb{E}_{\mathcal{D}} \left[\left(\frac{\mathbb{E}_{W|\mathcal{D}} W \cdot \mathbf{w}_{\text{erm}}}{d} \right) \left(\frac{\mathbb{E}_{W|\mathcal{D}} W \cdot \mathbf{w}_{\text{erm}}}{d} \right) \right] \quad (90)$$

$$= \mathbb{E}_{\mathcal{D}} \mathbb{E}_{W_1, W_2|\mathcal{D}} \left[\left(\frac{W_1 \cdot \mathbf{w}_{\text{erm}}}{d} \right) \left(\frac{W_2 \cdot \mathbf{w}_{\text{erm}}}{d} \right) \right] \quad (91)$$

$$= \mathbb{E}_{\mathcal{D}, \mathbf{w}^*} \left[\left(\frac{\mathbf{w}^* \cdot \mathbf{w}_{\text{erm}}}{d} \right) \left(\frac{\mathbb{E}_{W|\mathcal{D}} W \cdot \mathbf{w}_{\text{erm}}}{d} \right) \right] \quad (92)$$

$$= \mathbb{E}_{\mathcal{D}, \mathbf{w}^*} \left[\left(\frac{\mathbf{w}^* \cdot \mathbf{w}_{\text{erm}}}{d} \right) \left(\frac{\mathbf{w}_{\text{bo}} \cdot \mathbf{w}_{\text{erm}}}{d} \right) \right] \quad (93)$$

Then, from Cauchy-Schwartz we have

$$\mathbb{E} \left[\left(\frac{\mathbf{w}_{\text{bo}} \cdot \mathbf{w}_{\text{erm}}}{d} \right)^2 \right]^2 \leq \mathbb{E} \left[\left(\frac{\mathbf{w}_{\text{bo}} \cdot \mathbf{w}_{\text{erm}}}{d} \right)^2 \right] \mathbb{E} \left[\left(\frac{\mathbf{w}^* \cdot \mathbf{w}_{\text{erm}}}{d} \right)^2 \right] \quad (94)$$

$$\mathbb{E} \left[\left(\frac{\mathbf{w}_{\text{bo}} \cdot \mathbf{w}_{\text{erm}}}{d} \right)^2 \right] \leq \mathbb{E} \left[\left(\frac{\mathbf{w}^* \cdot \mathbf{w}_{\text{erm}}}{d} \right)^2 \right] \quad (95)$$

and as $d \rightarrow \infty$, we can use the concentration of the right hand side to m to obtain

$$\lim_{d \rightarrow \infty} \mathbb{E} \left[\left(\frac{\mathbf{w}_{\text{bo}} \cdot \mathbf{w}_{\text{erm}}}{d} \right)^2 \right] \leq m^2 \quad (96)$$

so that, given the second moment has to be larger or equal to its (squared) mean:

$$\lim_{d \rightarrow \infty} \mathbb{E} \left[\left(\frac{\mathbf{w}_{\text{bo}} \cdot \mathbf{w}_{\text{erm}}}{d} \right)^2 \right] = m^2 \quad (97)$$

□

We have thus proven that the overlap Q concentrates in quadratic mean to m as $d \rightarrow \infty$: with high probability, it is thus asymptotically equal to m . We shall now prove that \mathbf{w}_{bo} can be approximated by \mathbf{w}_{amp} . In fact, given the concentration of overlap, it will be enough to prove that :

$$\lim_{d \rightarrow \infty} \mathbb{E}_{\mathcal{D}_d} \frac{\hat{\mathbf{w}}_{\text{amp}}(\mathcal{D}_d) \cdot \mathbf{w}_{\text{erm}}(\mathcal{D})}{d} = \lim_{d \rightarrow \infty} \mathbb{E}_{\mathcal{D}_d} \frac{\hat{\mathbf{w}}_{\text{bo}}(\mathcal{D}_d) \cdot \mathbf{w}_{\text{erm}}(\mathcal{D})}{d} \quad (98)$$

This can be done in two steps. First, similarly as in section B.1, we use the fact that GAMP achieves Bayes optimality for the estimation of W^* [9]. This leads to the following lemma

Lemma B.8 (Bounds on differences of estimators for \mathbf{w}).

$$\lim_{d \rightarrow \infty} \mathbb{E}_{\mathcal{D}} \frac{\|\mathbf{w}_{\text{amp}} - \mathbf{w}_{\text{bo}}\|_2^2}{d} \rightarrow 0 \quad (99)$$

Proof. The proof proceed similarly as in lemma B.2. Denoting $\delta\mathbf{w}(\mathcal{D}) = \mathbf{w}_{\text{amp}}(\mathcal{D}) - \mathbf{w}_{\text{bo}}(\mathcal{D})$ we write

$$\mathbb{E}_{\mathcal{D}, \mathbf{W}^*} \frac{\|\mathbf{w}_{\text{amp}}(\mathcal{D}) - \mathbf{w}^*\|_2^2}{d} = \mathbb{E}_{\mathcal{D}, \mathbf{W}^*} \frac{\|\mathbf{w}_{\text{bo}}(\mathcal{D}) + \delta\mathbf{w}(\mathcal{D}) - \mathbf{w}^*\|_2^2}{d} \quad (100)$$

$$\begin{aligned} &= \mathbb{E}_{\mathcal{D}, \mathbf{W}^*} \frac{\|\mathbf{w}_{\text{bo}}(\mathcal{D}) - \mathbf{w}^*\|_2^2}{d} + \mathbb{E}_{\mathcal{D}} \frac{\|\delta\mathbf{w}(\mathcal{D})\|_2^2}{d} + \frac{1}{d} 2 \mathbb{E}_{\mathcal{D}} \mathbb{E}_{\mathbf{w}^* | \mathcal{D}} [\delta\mathbf{w}(\mathcal{D}) (\mathbf{w}^* - \mathbf{w}_{\text{bo}})] \\ &= \mathbb{E}_{\mathcal{D}} \frac{\|\delta\mathbf{w}(\mathcal{D})\|_2^2}{d} \end{aligned} \quad (102)$$

Using the optimality of GAMP for the MMSE yields the lemma. □

We can now prove the equality of overlaps

Lemma B.9.

$$\lim_{d \rightarrow \infty} \mathbb{E}_{\mathcal{D}_d} \frac{\hat{\mathbf{w}}_{\text{amp}}(\mathcal{D}_d) \cdot \mathbf{V}(\mathcal{D})}{d} = \lim_{d \rightarrow \infty} \mathbb{E}_{\mathcal{D}_d} \frac{\hat{\mathbf{w}}_{\text{bo}}(\mathcal{D}_d) \cdot \mathbf{V}(\mathcal{D})}{d} \quad (103)$$

Proof. The proof is an application of Cauchy-Schwartz inequality:

$$\left| \mathbb{E}_{\mathcal{D}_d} \frac{\hat{\mathbf{w}}_{\text{amp}}(\mathcal{D}_d) \cdot \mathbf{V}(\mathcal{D})}{d} - \mathbb{E}_{\mathcal{D}_d} \frac{\hat{\mathbf{w}}_{\text{bo}}(\mathcal{D}_d) \cdot \mathbf{V}(\mathcal{D})}{d} \right| = \left| \mathbb{E}_{\mathcal{D}_d} \left[\frac{(\hat{\mathbf{w}}_{\text{amp}} - \hat{\mathbf{w}}_{\text{bo}})(\mathcal{D}_d) \cdot \mathbf{V}(\mathcal{D})}{d} \right] \right| \quad (104)$$

$$\leq \sqrt{\mathbb{E} \frac{\|\mathbf{V}\|_2^2}{d} \mathbb{E} \frac{\|\mathbf{w}_{\text{bo}} - \mathbf{w}_{\text{amp}}\|_2^2}{d}} \quad (105)$$

taking the limit $d \rightarrow \infty$ yields the lemma. □

Applying the lemma to the ERM estimator, and using the concentration of overlaps, finally leads to

Lemma B.10 (Asymptotic Joint distribution of pre-activation). *Asymptotically, and with high probability over data, the joint distribution of pre-activation is asymptotically given by*

$$\lim_{d \rightarrow \infty} \mathbb{P}(\nu, \lambda, \lambda) = \mathcal{N} \left(0, \begin{pmatrix} \rho & q_{\text{bo}} & m \\ q_{\text{bo}} & q_{\text{bo}} & m \\ m & m & q_{\text{erm}} \end{pmatrix} \right) \quad (106)$$

An application of the change of variable formula then gives Theorem 3.2.

B.3 Proof of Theorem 3.3

Proof of Equation 23 Consider the local fields $(\nu, \lambda_{\text{erm}}, \lambda_{\text{amp}})$ defined in Equation (20). They follow a Gaussian distribution with covariance matrix Σ given in Equation (13). Then, $(\nu, \lambda_{\text{erm}})$ follows a bivariate Gaussian and the density of ν conditioned on $\hat{f}_{\text{erm}}(\mathbf{x}) = p$ follows the Gaussian distribution with mean $\mu = \frac{m}{q_{\text{erm}}} \sigma^{-1}(p)$ and variance $v^2 = \rho - \frac{m^2}{q_{\text{erm}}}$. Then,

$$\mathbb{E}_{\mathbf{x}} \left[f_{\star}(\mathbf{x}) | \hat{f}_{\text{erm}}(\mathbf{x}) = p \right] = \int d\nu \frac{1}{2} \text{erfc} \left(-\frac{\nu}{\sqrt{2\tau^2}} \right) \mathcal{N}(\nu | \mu, v^2) \quad (107)$$

$$= \frac{1}{2} \text{erfc} \left(-\frac{\mu}{\sqrt{2(\tau^2 + v^2)}} \right) = \frac{1}{2} \text{erfc} \left(-\frac{\frac{m}{q_{\text{erm}}} \sigma^{-1}(p)}{\sqrt{2(1 - \frac{m^2}{q_{\text{erm}}} + \tau^2)}} \right) \quad (108)$$

$$= \sigma_{\star} \left(-\frac{\frac{m}{q_{\text{erm}}} \sigma^{-1}(p)}{\sqrt{1 - \frac{m^2}{q_{\text{erm}}} + \tau^2}} \right) \quad (109)$$

which yields Equation 23. We used the property that, for any a, b ,

$$\int \text{erf}(ax + b) \mathcal{N}(x | \mu, \sigma^2) dx = \text{erf} \left(\frac{a\mu + b}{\sqrt{1 + 2a^2\sigma^2}} \right) \quad (110)$$

Proof of Equation 24 We use the same computation as in the previous paragraph: since the conditioned on the Bayes local field $\hat{f}_{\text{bo}}(\mathbf{x}) = \sigma_{\star} \left(\frac{\lambda_{\text{amp}}}{\sqrt{\tau^2 + 1 - q_{\text{bo}}}} \right) = p$, the teacher local field is Gaussian with mean $\mu = \sqrt{\tau^2 + 1 - q_{\text{bo}}} \sigma_{\star}^{-1}(p)$ and variance $v^2 = 1 - q_{\text{bo}}$. As before, we have

$$\mathbb{E}_{\mathbf{x}} \left[f_{\star}(\mathbf{x}) | \hat{f}_{\text{bo}}(\mathbf{x}) = p \right] = \sigma_{\star} \left(-\frac{\mu}{\sqrt{\tau^2 + v^2}} \right) \quad (111)$$

$$= \sigma_{\star} \left(-\frac{\sqrt{\tau^2 + 1 - q_{\text{bo}}} \sigma_{\star}^{-1}(p)}{\sqrt{\tau^2 + 1 - q_{\text{bo}}}} \right) = p \quad (112)$$

Hence the result of Equation 24.

Proof of Equation 25 The proof follows the same structure as the previous paragraphs: conditioned on $\sigma(\lambda_{\text{amp}}) = p$, the law of λ_{amp} is $\mathcal{N}(\frac{m}{q_{\text{erm}}} \sigma^{-1}(p), q_{\text{bo}} - \frac{m^2}{q_{\text{erm}}})$ and

$$\mathbb{E}_{\mathbf{x}} \left[\hat{f}_{\text{bo}}(\mathbf{x}) | \hat{f}_{\text{erm}}(\mathbf{x}) = p \right] = \int \sigma_{\star} \left(\frac{-x}{\sqrt{\tau^2 + 1 - q}} \right) \mathcal{N}(x | \frac{m}{q_{\text{erm}}} \sigma^{-1}(p), q_{\text{bo}} - \frac{m^2}{q_{\text{erm}}}) \quad (113)$$

$$= \sigma_{\star} \left(-\frac{\frac{m}{q_{\text{erm}}} \sigma^{-1}(p)}{\sqrt{\tau^2 + 1 - q_{\text{bo}} + (q_{\text{bo}} - \frac{m}{q_{\text{erm}}})}} \right) \quad (114)$$

$$= \left(-\frac{\frac{m}{q_{\text{erm}}} \sigma^{-1}(p)}{\sqrt{1 - \frac{m^2}{q_{\text{erm}}} + \tau^2}} \right) = \mathbb{E}_{\mathbf{x}} \left[f_{\star}(\mathbf{x}) | \hat{f}_{\text{erm}}(\mathbf{x}) = p \right] \quad (115)$$

Hence the result.

C Additional figures

C.1 Logistic regression uncertainty supplement

Figure 8 complements Figure 3 from the main text by showing the same plot as the right panel in Figure 3 for other values of sample complexity α and noise τ . We observe that at zero regularization the logistic regression is overconfident in all the depicted cases, in particular so at small α and small noise.

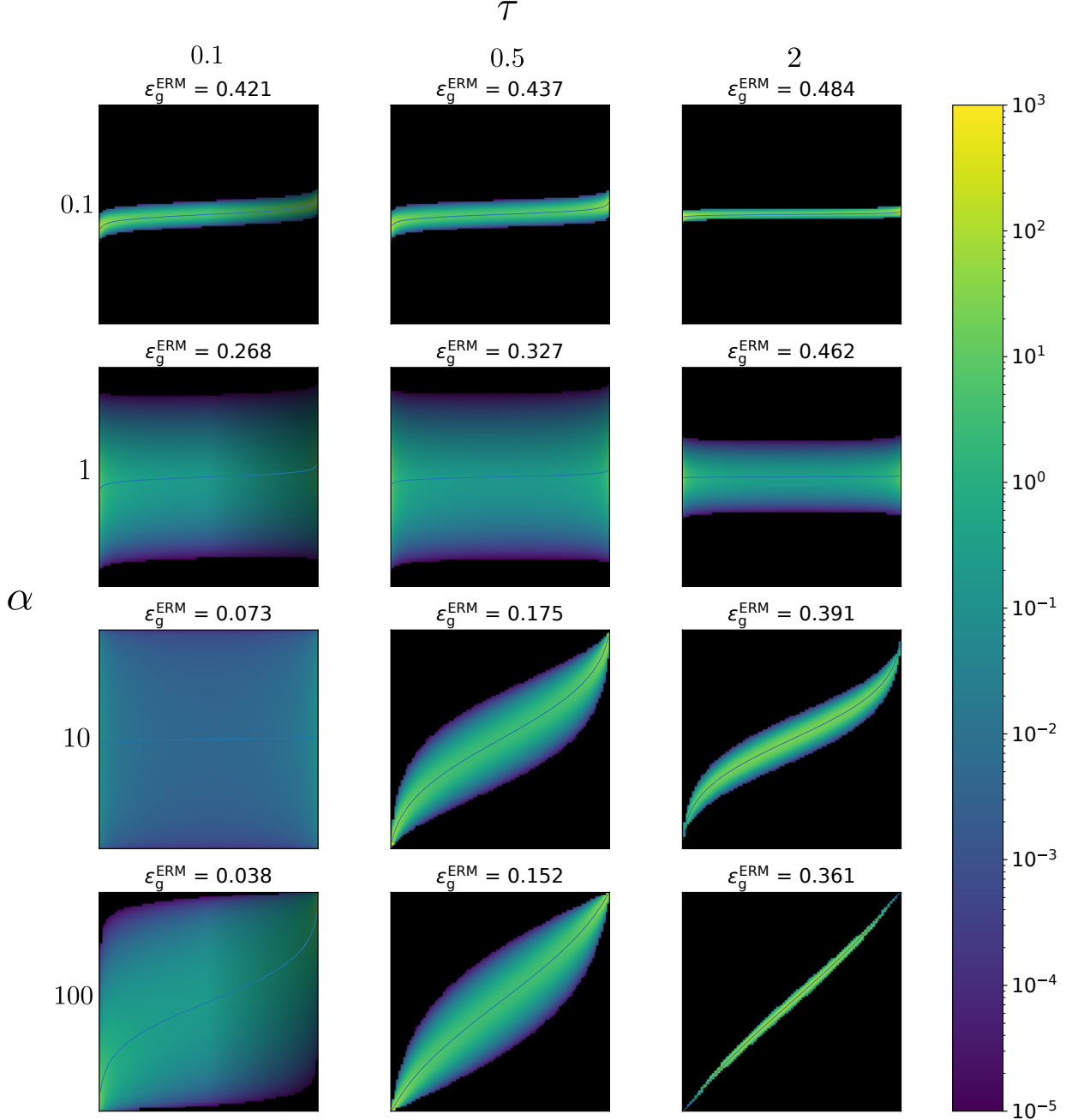


Figure 8: Joint density of \hat{f}_{erm} (x-axis) and \hat{f}_{bo} (y-axis), at $\lambda = 0$. Blue curve is the mean of \hat{f}_{bo} at fixed \hat{f}_{erm} . The test error of ERM is indicated above the corresponding plot. The test errors of Bayes for the same parameters are indicated in figure 2.

C.2 Choosing optimal regularization supplement

Here we give additional illustration related to the section 4.3 in the Main text. The left panel of figure 9 compares λ_{error} and λ_{loss} when $\tau = 0.5$. It appears there that in the range of α considered, $\lambda_{\text{loss}} > \lambda_{\text{error}}$. However, this inequality is not true in general. For example, at $\alpha = 100$, $\tau = 0.5$, $\lambda_{\text{loss}} = 1.570$ and $\lambda_{\text{error}} = 1.573$.

Figure 10 then shows that the test error at λ_{loss} and λ_{error} are extremely close, with the difference being plot in the inset.

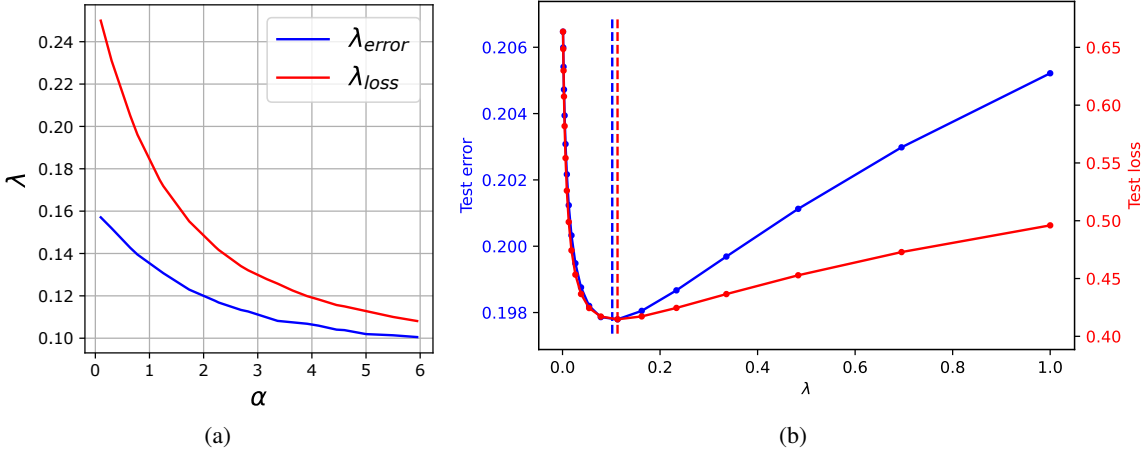


Figure 9: Left: optimal penalization for logistic regression as a function of the sample complexity α , for $\tau = 0.5$. Right: generalisation loss and error as a function of λ for $\alpha = 5, \tau = 0.5$.

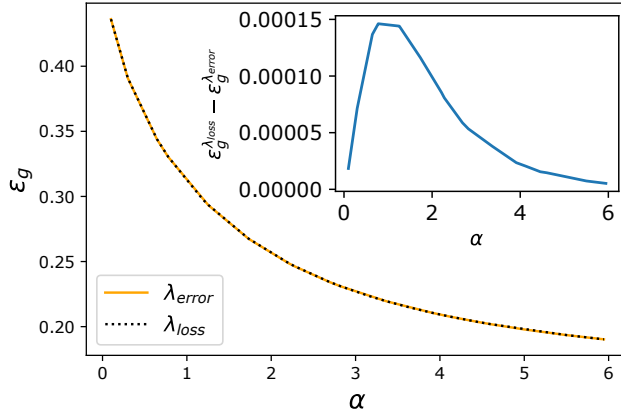


Figure 10: Test error at optimal λ for $\sigma = 0.5$, as a function of α . Orange line (respectively black dotted line) corresponds to λ -error (respectively λ -loss). The two curves are indistinguishable on the plot. The blue curve in the inset shows $\varepsilon_g^{\lambda_{\text{loss}}} - \varepsilon_g^{\lambda_{\text{error}}}$ as a function of α : it appears that the difference is around $\sim 10^{-4}$.

Figure 11 depicts the joint density of \hat{f}_{erm} (x-axis) and \hat{f}_{bo} (y-axis) for several values of the regularization λ and the noise τ . As λ increases, we observe that the logistic regression changes from overconfident to underconfident, as we could also observe in figure 7.

Next in Figures 12 and 13 we further corroborate the claim that logistic regression run at λ_{error} improves both the test error and the calibration with respect to $\lambda = 0$. Further at λ_{loss} the calibration is even better without loosing much on the test error. Compare visually Figure 12 for λ_{error} , and Figure 13 for λ_{loss} to the Figure 8 for $\lambda = 0$. We see the the calibration line is clearly improved (closer $y = x$) with respect to the non-regularized regression.

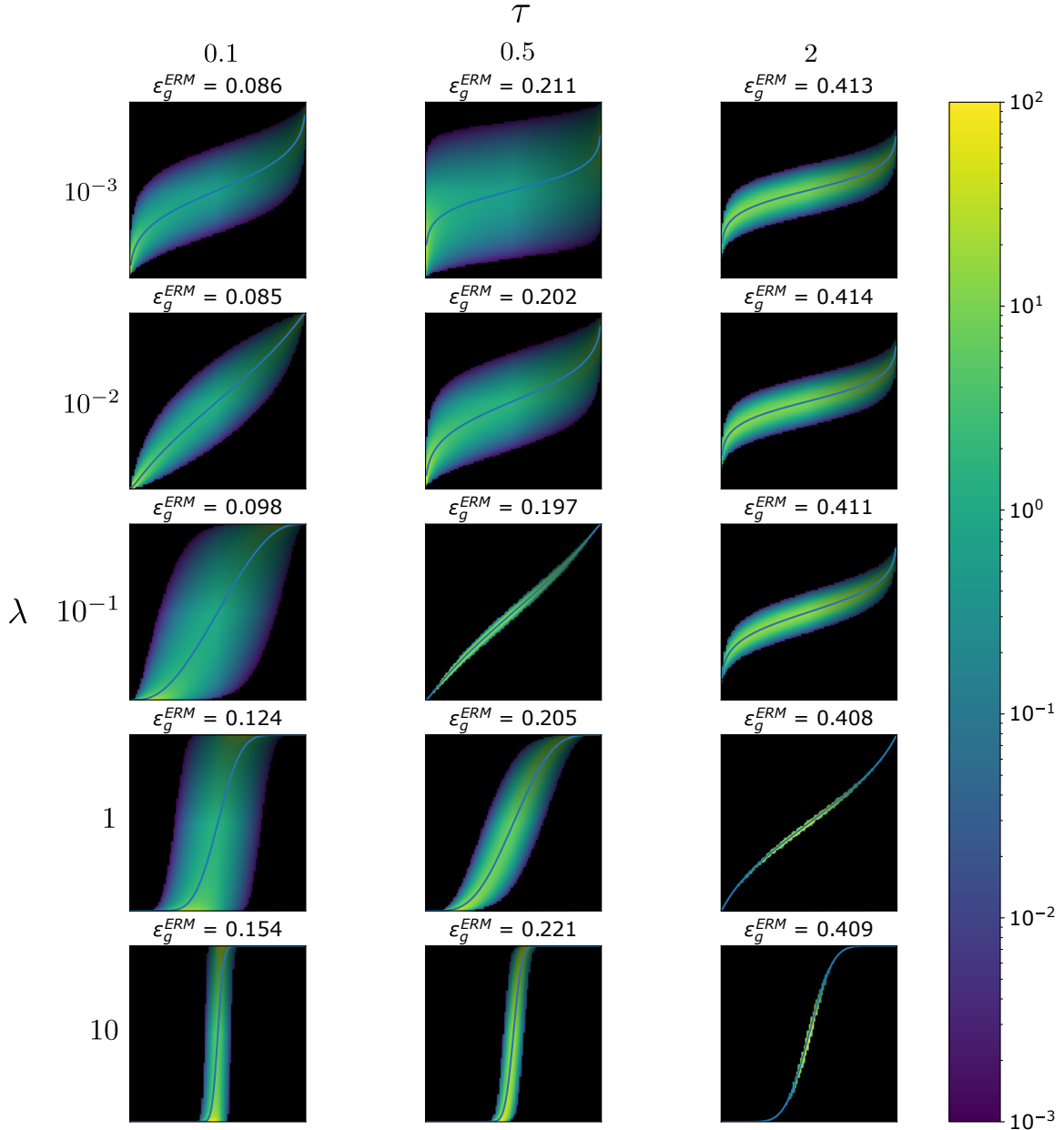


Figure 11: Joint density of \hat{f}_{erm} (x-axis) and \hat{f}_{bo} (y-axis) at $\alpha = 5$. The best possible test errors are respectively $\varepsilon_g^* = 0, 0.148, 0.352$ for $\tau = 0, 0.5, 2$. For the Bayes estimator with $\alpha = 5$, the test errors are $\varepsilon_g^{\text{bo}} = 0.083, 0.198, 0.402$

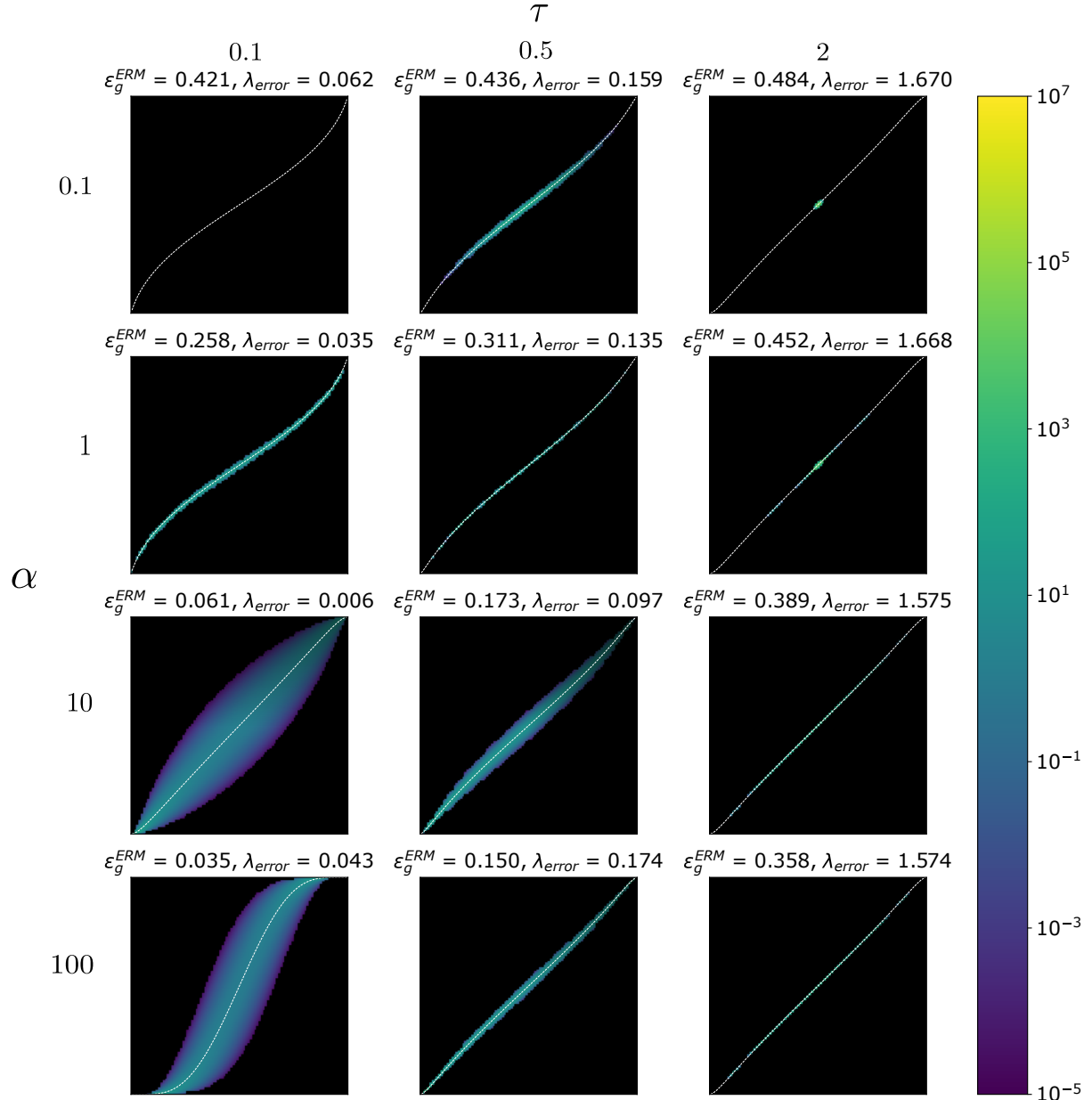


Figure 12: Joint density $\rho_{\text{perm,bo}}$, at $\lambda = \lambda_{\text{error}}$. λ_{error} and the test error of ERM are indicated above the corresponding plot.

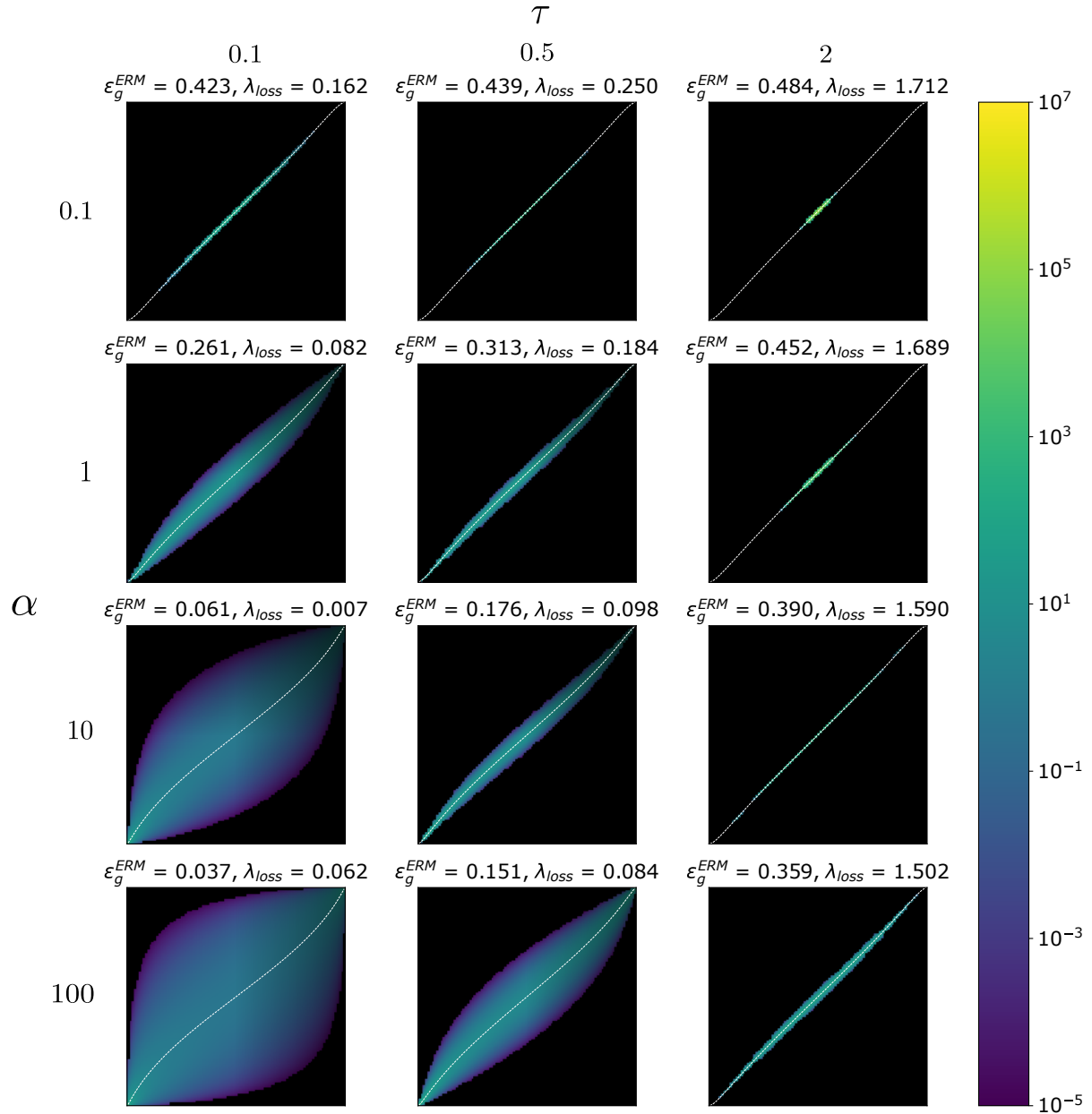


Figure 13: Joint density $\rho_{\text{erm,bo}}$, at $\lambda = \lambda_{\text{loss}}$. λ_{loss} and the test error of ERM are indicated above the corresponding plot.